Dynamics of Negatively Refracted Light in Tilings

Kelsey DiPietro, Jenny Rustad, Alexander St Laurent

June 26, 2014

Abstract

In this paper we study the properties of trajectories of light negatively refracted in three families of tilings. In particular, we examine divisions of the plane by a finite number of lines, in addition to triangle tilings and the trihexagonal tiling. In each of these cases we study the existence and stability of periodic orbits as well as boundedness of trajectories in the case of triangle tilings.

1 Introduction

When light travels from one medium to another, the path of the light may bend; this bending is known as refraction. *Snell's law* describes the change in angle of the path, relating it to the indices of refraction of the two media.

In nature, the indices of refraction of all materials are positive. However, physicists have recently created materials, called "metamaterials," with *negative* indices of refraction [1]. Refractions across the boundary between a medium with a positive index and a negative index cause the light to bend in the opposite direction as it would passing between two media with positive indices. In particular, we consider light passing from a medium with index $+n$ to a medium of index $-n$ so that the angle of refraction is "reflected" across the interface. In this way, we define trajectories through two-colorable tilings (where each color corresponds to an index of refraction). In fact, we will ignore the colorability requirement as to define such trajectories through any tiling, or any division of the plane by boundary lines.

If a trajectory returns to its initial location at its initial angle, we call that trajectory *periodic*. In tilings with translational symmetry, if the trajectory is periodic up to translation, we call that trajectory *drift periodic*. For we both, may use the term *orbit* instead of trajectory. If a trajectory is either periodic or drift-periodic, we also check for stability. A *stable* trajectory maintains periodicity under perturbations of the angle or parallel translations.

When looking at tilings, we look for the existence of drift-periodic and periodic trajectories. We want to know how many, if any, of these trajectories exist, the conditions for existence and their stability. We studied the previous questions in the following instances: n lines meeting to form an n-gon (and n lines meeting at a point), triangle tilings, and the trihexagonal tiling.

When n lines meet to form an n-gon with no parallel edges, then if n is odd, then there exists an unstable periodic orbit, while if n is even, then there exists a stable periodic orbit if $(\alpha_{n-2}-\alpha_{n-1})+\cdots+(\alpha_2-\alpha_3)+(\alpha_0-\alpha_1)=0$ (Thm. 2.13, Prop. 2.16). These theorems will hold if the size of the n-gon is zero, i.e. we have n lines meeting at a point.

In isosceles triangle tilings, we find that every orbit is either periodic or drift-periodic with maximum drift period $2n+2$ and maximum period $2n+4$, where $n \in \mathbb{N}$ depends on the vertex angle of the tiling and initial angle of the orbit (Prop. 3.4).

In right triangle tilings, we find that if an orbit bisects a hypotenuse, then the orbit is unbounded (Prop. 3.7); this orbit is stable under perturbation from the midpoint if the acute angles of the tiling triangle are rational multiples of π (Prop. 3.9). If the smallest angle of a tiling triangle is $\frac{\pi}{2}$, then there exists a drift-periodic orbit (Prop. 3.10). We also conjecture that in such a tiling, any orbit

starting in a right corner will meet a second right corner; so far, it has been proven that it depends only on the tiling triangle whether an orbit connects two corners (Lemma **??**).

When we study triangle tilings in general, we find that in any triangle tiling, except tilings of isosceles triangles with vertex angle greater than or equal to $\frac{\pi}{3}$, there exists a ten-periodic orbit.

In the trihexagonal tiling, we encounter three different trajectory paths common to our orbits. Lemmas 4.1,4.2, and 4.4 define these trajectory paths that are useful in proofs of theorems.

We also find three periodic trajectories, as seen in Theorems 22,4.7, 4.17. The initial angle for each of these periodic trajectories is $\alpha = \frac{\pi}{2}, \alpha = \frac{\pi}{3}$, and $\alpha = \pi - \tan^{-1}(2\sqrt{3})$, respectively. All three of the trajectories in these theorems are unstable under angle pertubations. However, the trajectories described in Theorems 4.5 and 4.7 are stable under parallel translations, except when the trajectory passes through the center of a hexagon.

After using trigonometric arguments to prove the existence of the three periodic trajectories, we move on to finding drift-periodic trajectories. We prove the existence of two drift-periodic trajectories in Theorems 4.11 and **??**. The initial angle for these drift-periodic trajectories is $\alpha = \pi - \tan^{-1}(6n - 3\sqrt{3})$ and $\alpha = \pi - \tan^{-1}(\frac{3n\sqrt{3}}{3n-2})$, respectively, where $n \in \mathbb{N}$. This gives us two families of drift-periodic trajectories, one that converges to the 6-periodic orbit (Theorem 4.14) and the other that converges to the 12-periodic orbit (Theorem 4.11). Like the periodic orbits, these drift-periodic orbits are unstable under angle pertubations and stable under parallel translations.

In the future, we will be looking for other periodic orbits. From experimental results, there seem to be families of periodic orbits that are unstable under both parallel translations and angle shifts. Our next step will be proving the existence of such periodic orbits and finding classifications for each of them.

1.1 Physical Significance

Negative refraction was once a theoretical fantasy. Recently, however, physicists have created media that negatively refract light, called "metamaterials." These new materials may someday be used to create an invisibility shield, improve solar panel technology, or fabricate a perfect lens that would be able to resolve details even smaller than the wavelengths of light used to create the image [3]. Since metamaterials are not found in nature, we have little intuition for their effects on light in complex scenarios. To remedy this, our research studies tilings of metamaterials to illustrate trends in the behavior of light refracted by metamaterials. This problem is also similar to polygonal inner billiards, except that at each interface, light is reflected across the boundary instead of across the normal to the boundary.

1.2 Previous Results

Mascarenhas and Fluegel asserted in [1] that every trajectory in the standard equilateral triangle tiling (meeting 6 to a vertex) is periodic, and every trajectory in a square tiling (meeting 4 to a vertex) is either periodic or drift periodic. These are easy to prove if we consider the fact that a line of reflective symmetry runs through every edge in each of these tilings.

In [2], Engelman and Kimball proved in the square tiling, where every other row is shifted by half of the square's side-length, that every trajectory is either periodic or drift periodic.

Additionally, Engelman and Kimball proved there is always a periodic orbit about the intersection of three lines (see Figure **??**), and there is no periodic orbit about the intersection of non-perpendicular two lines. This paper generalizes those results to the intersection of n lines for n odd and n even.

2 n Lines Meeting at an n-Gon

Definition 2.1. Let P_n be a convex n-gon in the plane with no parallel edges, and extend each of its edges into lines. The resulting figure is called a *P_n-star*. Without loss of generality, we may

assume that P_n has a horizontal edge, and that P_n lies above this edge. Let l_0 be the extension of the horizontal edge, and let $l_1, \ldots, l_{n-1}$ denote the rest of the edges, going clockwise (Figure 1).

Definition 2.2. The convex hull of the intersection points of a P_n-star is called the central zone. Because a P_n-star has a finite number of intersection points, the central zone is bounded.

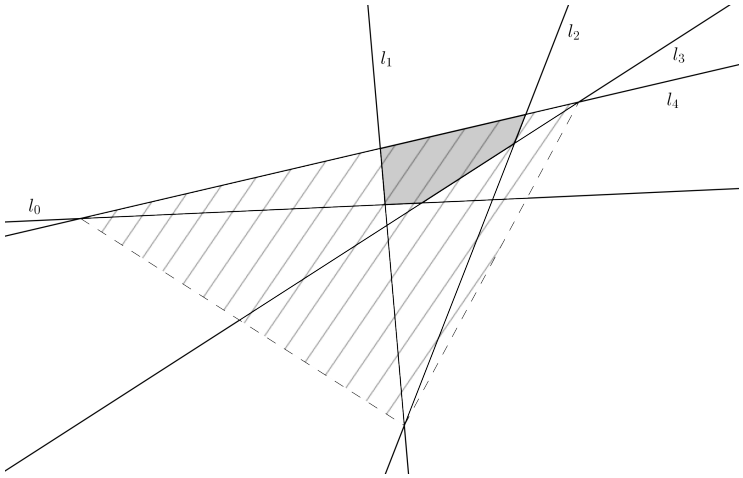

Figure 1: A P_5-star, where P_5 is the solidly shaded pentagon. The central zone is the hatched region.

We restrict our analysis to trajectories which remain outside the central zone. One might imagine "zooming out" from the figure above so that the polygon and central zone contract to a point—later, this intuition serves as motivation for extending our results to the case where n lines meet at a point.

Definition 2.3. Define the angle α_i for $i = 0, \ldots, n-1$ to be the clockwise angle between lines l_i and l_{i+1}, considering the indices mod n (Figure 2).

Lemma 2.4. $\alpha_0 + \alpha_1 + \cdots + \alpha_{n-1} = \pi$.

Proof. Parallel-translate each of the lines so that they all coincide at a single point (Figure 2). Then the result is clear.

□

Definition 2.5. In any division of the plane containing regions of infinite size, we say a trajectory *escapes* if it eventually remains in a single region, i.e. it stops refracting across lines.

Lemma 2.6. *Divide the plane by a P_n-star, and initiate a trajectory from l_0. As long as the trajectory neither enters the central zone nor escapes, it will cross the lines in numerical order: $l_0, l_1, \ldots, l_{n-1}, l_0, l_1$, etc.*

Proof. Assume the trajectory has just crossed l_i. There are four options: to enter the central zone, to escape, to re-cross l_i, or to cross l_{i+1}. The first two options are impossible by assumption, and the third option is impossible because two lines can only intersect once in the plane. Thus, the trajectory must cross l_{i+1}. □

Definition 2.7. Divide the plane by a P_n-star. Initiate a trajectory from l_0 that is far enough away from P_n and at such an angle so that the trajectory both remains outside the central zone of the P_n-star and does not escape. We assume that every trajectory is given to us with an identified "starting point," p_0, and an initial angle, θ_0. Let p_i be the intersection point between the trajectory and the line it intersects at the i^{th} intersection and let θ_i be the angle between the trajectory and this line. (Note that this i^{th} intersection is with the line whose subscript is $i \pmod n$.) For convenience, we also define the functions $p_i(\tau) = p_i$, and $\theta_i(\tau) = \theta_i$, which give us the intersection point and

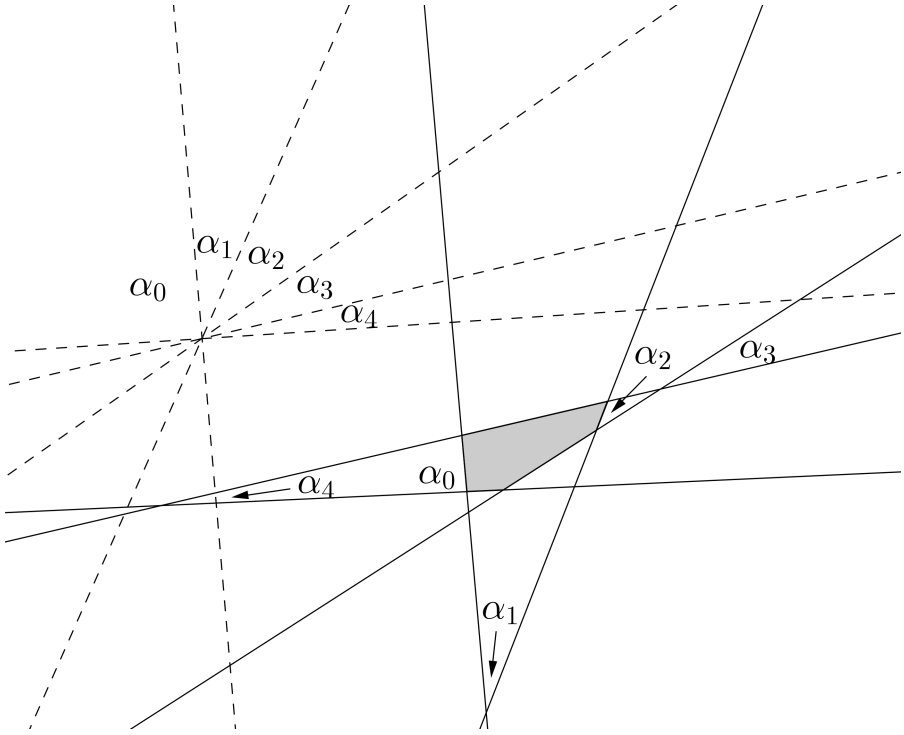

Figure 2: The angles α_i sum to π.

angle at the i^{th} intersection for a trajectory τ. Furthermore, consider triangles $p_{i-1}[l_{i-1} \cap l_i]p_i$ and $p_i[l_i \cap l_{i+1}]p_{i+1}$, where $\cap$ denotes the point of line intersection. Both of these triangles has an edge along l_i. Let x_i be the length of the shorter edge, and let $x_i + z_i$ be the length of the longer edge, so that z_i is the length of the segment between the respective intersections at α_{i-1} and α_i (Figure 3).

[Note to self/editor: is it even a thing to name triangles by their angles like that? It seems convenient here.]

2.1 Trajectories around a P_n-star that neither enter its central zone nor escape.

In all the results in this section, consider dividing the plane by a P_n-star that has no parallel lines. Initiate a trajectory from l_0 that is far enough away from the polygon P_n so that the trajectory does not enter the central zone of the P_n-star nor escapes for at least $2n$ iterations.

It is important to note that the requirement we stay outside the central zone isn't taxing: one can zoom out on the P_n-star until its central zone is of arbitrarily small size.

Lemma 2.8. *If $\theta_n = \theta_0$, then $\theta_{i+n} = \theta_i$ for all i with $0 \leq i \leq n$.*

Proof. The proof proceeds by induction. The base case is $\theta_n = \theta_0$, which is true by assumption. Next, assume $\theta_{k+n} = \theta_k$ for some k, $0 < k < n$. Then, because the trajectory forms a triangle with angles $\theta_k \alpha_k \theta_{k+1}$, as well as triangle $\theta_{k+n}\alpha_k\theta_{k+1+n}$ (Figure 4), it must be the case that $\theta_{k+n+1} = \theta_{k+1}$ (two triangles with two equal angles are similar). This inductive step is valid as long as the trajectory does not enter the central zone of the P_n-star. Therefore $\theta_{i+n} = \theta_i$ for all i with $0 \leq i \leq n$. □

For each triangle $T_i = \theta_i \alpha_i \theta_{i+1}$, let $x_i + p_i$ be the length of the edge of T_i which is along l_i (so $p_i = 0$ or $p_i = z_i$), and let $x_{i+1} + q_{i+1}$ be the length of the edge of T_i which is along l_{i+1} (so $q_{i+1} = 0$ or $q_{i+1} = z_{i+1}$)

Lemma 2.9. *For all $i, i = 0 \ldots n$, $p_i = q_{i+n}$ and $q_i = p_{i+n}$.*

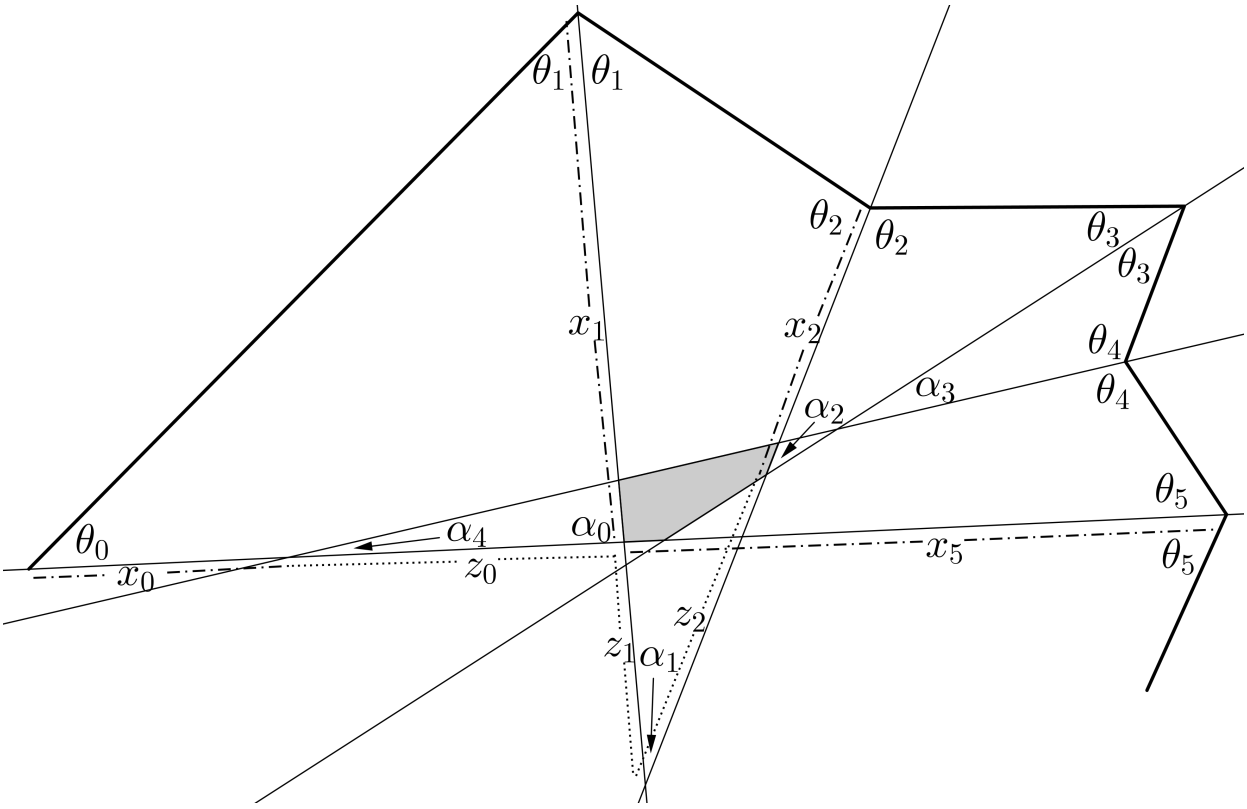

Figure 3: A P_5-star, where P_5 is the shaded convex pentagon. A trajectory is represented by the thick line.

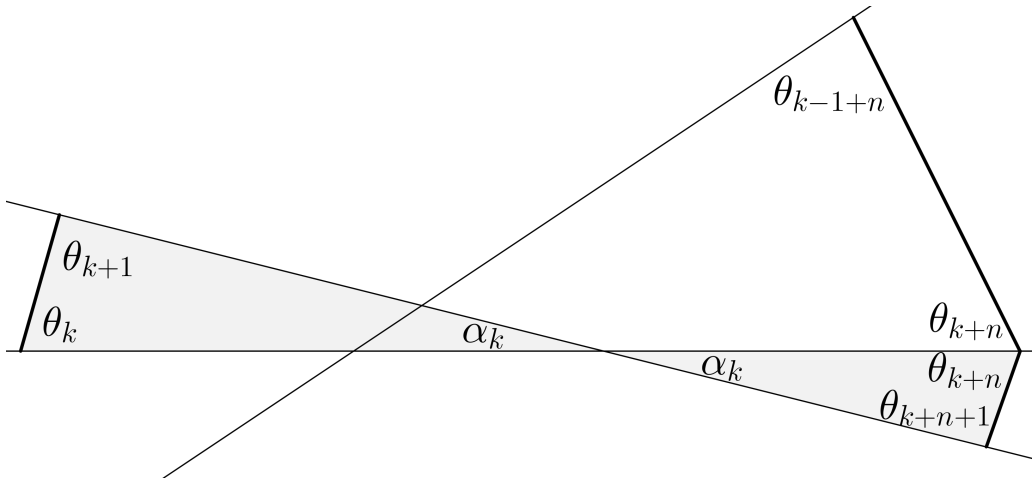

Figure 4: The trajectory forms similar triangles.

Proof. Without loss of generality, consider l_i to be horizontal with l_{i+1} and l_{i-1} intersecting above l_i (Figure 5). From triangle $T_i = \theta_i\alpha_i\theta_{i+1}$, we see that $p_i = z_i$. From triangle $T_{i-1+n} = \theta_{i-1+n}\alpha_{i-1}\theta_{i+n}$, we see that $q_{i+n} = z_i$. So $p_i = q_{i+n}$. From triangle $T_{i+n} = \theta_{i+n}\alpha_i\theta_{i+1+n}$, we see that $p_{i+n} = 0$. From triangle $T_{i-1} = \theta_{i-1}\alpha_{i-1}\theta_i$, we see that $q_i = 0$. So $q_i = p_{i+n}$.

The alternative is $p_i = q_{i+n} = 0$ and $q_i = p_{i+n} = z_i$. This occurs where l_{i-1} and l_{i+1} intersect below l_i. □

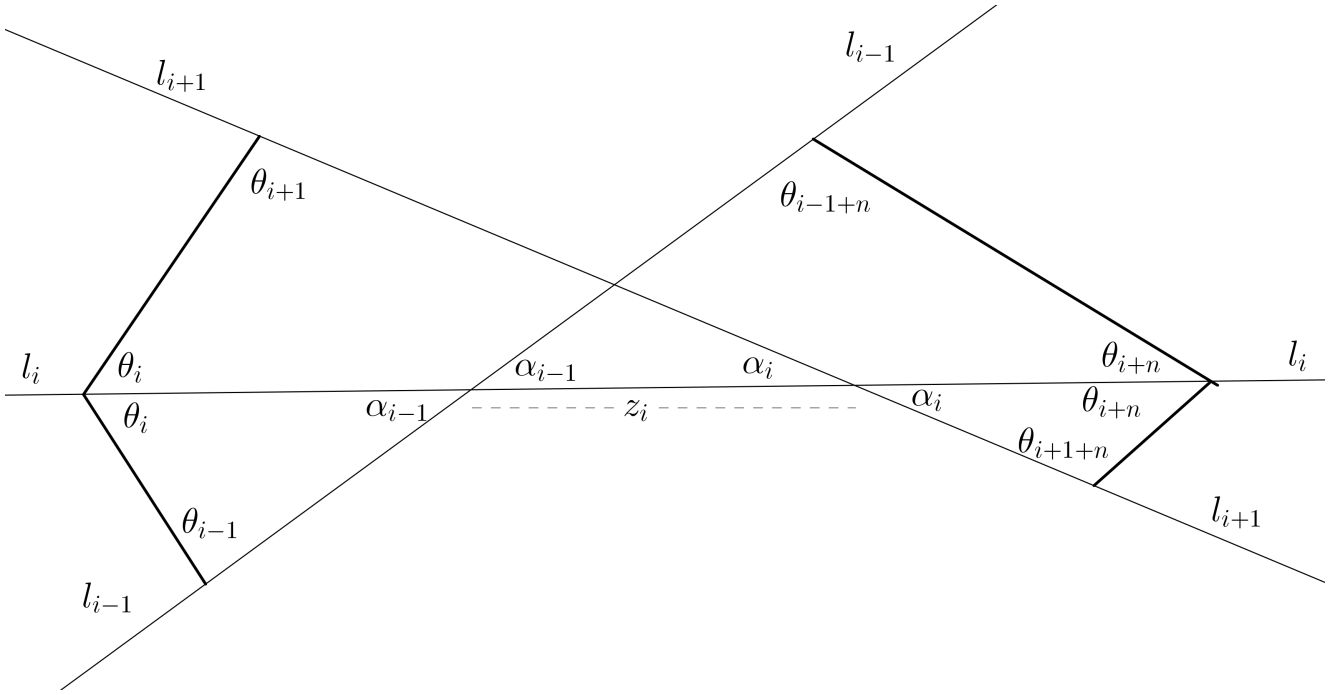

Figure 5: The subset of the trajectory around l_i.

Proposition 2.10. *If $\theta_n = \theta_0$, then the trajectory is periodic. If $\theta_n \neq \theta_0$, then $x_{2n} \neq x_0$.*

Proof. Because $\theta_{2n} = \theta_n$ by Lemma 2.8, which equals θ_0 by assumption, we have $\theta_{2n} = \theta_0$. Thus, to show periodicity, it sufficies to show $x_{2n} = x_0$.

In general, x_{i+1} can be expressed in terms of x_i via the law of sines.

The law of sines applied to T_i gives:

$$\begin{aligned}
\frac{x_{i+1} + q_{i+1}}{\sin\theta_i} &= \frac{x_i + p_i}{\sin\theta_{i+1}} \\
x_{i+1} &= \frac{\sin\theta_i}{\sin\theta_{i+1}}(x_i + p_i) - q_{i+1} \\
x_{i+1} &= \frac{\sin\theta_i}{\sin\theta_{i+1}} x_i + c_i
\end{aligned}$$

in which $c_i = \frac{\sin\theta_i}{\sin\theta_{i+1}} p_i - q_{i+1}$ depends strictly on $\theta_i, \theta_{i+1}, z_i, z_{i+1}$.

When we use this to replace x_{2n} with an expression involving x_0, we get:

$$
\begin{aligned}
x_{2n} &= \frac{\sin\theta_{2n-1}}{\sin\theta_{2n}}\left(\frac{\sin\theta_{2n-2}}{\sin\theta_{2n-1}}\left(\dots\left(\frac{\sin\theta_0}{\sin\theta_1}x_0 + c_0\right)\dots\right) + c_{2n-2}\right) + c_{2n-1} \\
&= \frac{\sin\theta_0}{\sin\theta_{2n}}x_0 + \left(\frac{\sin\theta_1}{\sin\theta_{2n}}c_0 + \frac{\sin\theta_2}{\sin\theta_{2n}}c_1 + \dots + \frac{\sin\theta_{2n}}{\sin\theta_{2n}}c_{2n-1}\right) \\
&= x_0 + \frac{1}{\sin\theta_{2n}}\sum_{i=0}^{2n-1}\sin\theta_{i+1}\left(\frac{\sin\theta_i}{\sin\theta_{i+1}}p_i - q_{i+1}\right) \\
&= x_0 + \frac{1}{\sin\theta_{2n}}\sum_{i=0}^{2n-1}\sin\theta_i p_i - \sin\theta_{i+1}q_{i+1} && (*) \\
&= x_0 + \frac{1}{\sin\theta_{2n}}\left(\sum_{i=0}^{2n-1}\sin\theta_i p_i - \sum_{j=1}^{2n}\sin\theta_j q_j\right) && (\theta_{i+n} = \theta_i) \\
&= x_0 + \frac{1}{\sin\theta_{2n}}\left(\sum_{i=0}^{n-1}\sin\theta_i(p_i + p_{i+n}) - \sum_{j=1}^{n}\sin\theta_j(q_i + q_{i+n})\right) \\
&= x_0 + \frac{1}{\sin\theta_{2n}}\left(\sin\theta_0(p_0 + p_n) + \sum_{i=1}^{n-1}\sin\theta_i(p_i - q_{i+n} + p_{i+n} - q_i) - \sin\theta_n(q_n + q_{2n})\right) \\
&= x_0 + \frac{1}{\sin\theta_{2n}}\left(\sin\theta_0(p_0 - q_n + p_n - q_{2n}) + \sum_{i=1}^{n-1}\sin\theta_i(p_i - q_{i+n} + p_{i+n} - q_i)\right) \\
&= x_0 && \text{(Lemma 2.9)}
\end{aligned}
$$

If $\theta_n \neq \theta_0$, then we have:

$$
\begin{aligned}
&= x_0 + \frac{1}{\sin\theta_{2n}}\sum_{i=0}^{2n-1}\sin\theta_i p_i - \sin\theta_{i+1}q_{i+1} && (\text{from}(*)) \\
&\neq x_0
\end{aligned}
$$

[Note to self/editor: With this method, I feel like I can only actually conclude that I cannot conclude $x_{2n} = x_0$, rather than explicitly concluding $x_{2n} \neq x_0$. I'm sure there's some argument I can make, but I'm not finding it at the moment. I know I can't say the extra term is always positive, or always negative, because it could be either.]

□

Definition 2.11. A periodic trajectory is *stable* if, when the initial angle is changed by some arbitrarily small angle ϵ, the the trajectory hits the same series of edges and the returns to its starting angle and location. If the trajectory hits different edges, or if it returns to a different location or at a different angle, we say the trajectory is *unstable*.

Proposition 2.12. *If $\theta_n = \theta_0$ with n even, the trajectory is periodic and stable. If $\theta_n = \theta_0$ with n odd, the trajectory is periodic and unstable; in this case, the perturbed trajectory spirals.*

Proof. Since $\theta_n = \theta_0$, the trajectory is periodic by Proposition 2.10, so it suffices to examine the stability.

Call our trajectory τ, with τ' denoting the trajectory whose initial angle is perturbed by ϵ, where ϵ is small enough so that τ' remains outside the central zone for $2n$ iterations.

Then we have $\theta_0(\tau') = \theta_0(\tau) + \epsilon$, $\theta_1(\tau') = \theta_1(\tau) - \epsilon$, $\theta_2(\tau') = \theta_2(\tau) + \epsilon$, etc. Whether n is odd or even, we have $\theta_{2n}(\tau') = \theta_{2n}(\tau) + \epsilon$ (because $2n$ is always even), thus returning the trajectory to the same angle.

If n is even, then $\theta_n(\tau') = \theta_n(\tau) + \epsilon = \theta_0(\tau')$. By Proposition 2.10, τ' is periodic, meaning τ is stable.

If n is odd, then $\theta_n(\tau') = \theta_n(\tau) - \epsilon = \theta_0(\tau') - 2\epsilon$. By Proposition 2.10, $x_{2n}(\tau') \neq x_0(\tau')$, so τ is unstable. But, since we still have $\theta_{2n} = \theta_0$, τ' spirals.

□

2.2 Constructing periodic around a P_n-star which does not enter its central zone

Proposition 2.12 gave a condition for a trajectory to periodic, and for it to be stable. In this section, we explicitly construct examples of periodic orbits around a P_n-star and analyze their stability.

Theorem 2.13. *Let $n \geq 3$ be odd. Fix a trajectory with*

$$\theta_0 = \alpha_1 + \alpha_3 + \cdots + \alpha_{n-2}$$

which initiates from l_0 in such a way that it does not enter the central zone for at least $2n$ iterations. Then the trajectory is periodic and unstable; the perturbed trajectory spirals.

Proof. For each triangle $\theta_{i-1}\alpha_{i-1}\theta_i$, the angles satisfy the recurrence relation:

$$\theta_i = \pi - (\alpha_{i-1} + \theta_{i-1})$$

Considering indices mod n, $\alpha_i + \alpha_{i+1} + \cdots + \alpha_{i+n-1} = \pi$ for any i. So, each time we compute a θ_i, we can treat the π term of the recurrence relation as the sum of α_ks from $k = i-1$ through $k = i+n-2$.

$$\begin{aligned}
\theta_0 &= \alpha_1 + \alpha_3 + \cdots + \alpha_{n-2} \\
\theta_1 &= \pi - (\alpha_0 + \theta_0) = (\alpha_0 + \cdots + \alpha_{n-1}) - (\alpha_0 + \theta_0) = \alpha_2 + \alpha_4 + \cdots + \alpha_{n-1} \\
\theta_2 &= \pi - (\alpha_1 + \theta_1) = (\alpha_1 + \cdots + \alpha_n) - (\alpha_1 + \theta_1) = \alpha_3 + \alpha_5 + \cdots + \alpha_n \\
&\vdots \\
\theta_{n-1} &= \pi - (\alpha_{n-2} + \theta_{n-2}) = (\alpha_{n-2} + \cdots + \alpha_{2n-3}) - (\alpha_{n-2} + \theta_{n-2}) = \alpha_n + \alpha_{n+2} + \cdots + \alpha_{2n-3} \\
\theta_n &= \pi - (\alpha_{n-1} + \theta_{n-1}) = (\alpha_{n-1} + \cdots + \alpha_{2n-2}) - (\alpha_{n-1} + \theta_{n-1}) = \alpha_{n+1} + \alpha_{n+3} + \cdots + \alpha_{2n-2} \\
&= \alpha_1 + \alpha_3 + \cdots + \alpha_{n-2} \\
&= \theta_0
\end{aligned}$$

Because $\theta_n = \theta_0$, we have $\theta_{i+n} = \theta_i$ for $i = 0, \ldots, n$ by Lemma 2.8. Because $0 < \theta_0, \ldots, \theta_{2n} < \pi$, we know that the trajectory does not escape for at least $2n$ iterations. Because of this, and because $\theta_n = \theta_0$, then by Proposition 2.12, the trajectory is periodic and unstable; the perturbed trajectory spirals. □

Corollary 2.14. *Let $n \geq 3$ be odd. Divide the plane by an P_n-star, where P_n is a regular n-gon. There is an unstable periodic orbit remaining outside the central zone with $\theta_0 = \frac{(n-1)}{2n}\pi$.*

Proof. Because n is odd, P_n does not have any parallel edges. Because of this the P_n-star does have no parallel lines. By Theorem 2.13, there is an unstable periodic orbit remaining outside the central zone, with $\theta_0 = \alpha_1 + \alpha_3 + \cdots + \alpha_{n-2}$.

By symmetry, $\alpha_i = \alpha_0$ for all i, sp $\alpha_0 = \frac{\pi}{n}$ (Lemma 2.4). Thus, $\theta_0 = \frac{(n-1)}{2}\alpha_0 = \frac{(n-1)}{2n}\pi$. □

Lemma 2.15. *Let $n \geq 4$ be even. Assuming the trajectory does not escape, then*

$$\theta_{i+n} = (\alpha_{i+n-2} - \alpha_{i+n-1}) + (\alpha_{i+n-4} - \alpha_{i+n-3}) + \cdots + (\alpha_i - \alpha_{i+1}) + \theta_i$$

Proof. First, we determine a relation between θ_{i+n} and θ_{i+n-2}. By the fact that the internal angles of a triangle sum to π, we have:

$$\begin{aligned}
\theta_{i+n} &= \pi - \alpha_{i+n-1} - \theta_{i+n-1} \\
&= \pi - \alpha_{i+n-1} - (\pi - \alpha_{i+n-2} - \theta_{i+n-2}) \\
&= (\alpha_{i+n-2} - \alpha_{i+n-1}) + \theta_{i+n-2}
\end{aligned}$$

Next, because n is even, we can apply this relation $\frac{n}{2}$ times until we have a relation between θ_{i+n} and θ_i, thus arriving at the statement of the Lemma:

$$\begin{aligned}\theta_{i+n} &= (\alpha_{i+n-2} - \alpha_{i+n-1}) + \theta_{i+n-2} \\ &= (\alpha_{i+n-2} - \alpha_{i+n-1}) + (\alpha_{i+n-4} - \alpha_{i+n-3}) + \theta_{i+n-4} \\ &= \vdots \\ &= (\alpha_{i+n-2} - \alpha_{i+n-1}) + \cdots + (\alpha_i - \alpha_{i+1}) + \theta_i\end{aligned}$$

□

Theorem 2.16. *Let $n \geq 4$ be even. Fix a P_n-star with*

$$(\alpha_{n-2} - \alpha_{n-1}) + \cdots + (\alpha_2 - \alpha_3) + (\alpha_0 - \alpha_1) = 0$$

Initiate a trajectory from l_0 in such a way that it does not enter the central zone for at least $2n$ iterations. Then, it is periodic and stable. If the condition on the α_is is not satisfied, then every trajectory must either enter the central zone or escape.

Proof. From Lemma 2.15, we have

$$\theta_{i+n} = (\alpha_{i+n-2} - \alpha_{i+n-1}) + (\alpha_{i+n-4} - \alpha_{i+n-3}) + \cdots + (\alpha_i - \alpha_{i+1}) + \theta_i$$

Letting $\beta = (\alpha_{n-2} - \alpha_{n-1}) + \cdots + (\alpha_2 - \alpha_3) + (\alpha_0 - \alpha_1)$, we get $\theta_n = \beta + \theta_0$. So, if $\beta = 0$, $\theta_n = \theta_0$. By Proposition 2.12, the trajectory is periodic and stable.

If $\beta \neq 0$, then $\{\theta_0, \theta_n, \theta_{2n}, \dots\}$ is either an increasing or a decreasing sequence, depending on the sign of β. If $\beta > 0$, then this sequence eventually surpasses π. If $\beta < 0$, the sequence eventually surpasses 0. In either case, the trajectory must either escape or enter the central zone. □

Remark 2.17. If we let entire central zone of the P_n-star shrink to a point, and the limiting case of the figure is n-lines meeting at a point, preserving the angles α_i. In this process, the $z_i \to 0$, so the amount by which x_{2n} differs from x_n approaches 0. The limiting case of all periodic orbits about P_n-stars are *stable* periodic orbits about n coincident lines. This culminates in the following theorem.

Theorem 2.18. *Divide the plane by n lines $l_0, \dots, l_{n-1}$ intersecting at a point p, forming angles $\alpha_0, \dots, \alpha_{n-1}$. Initiate a trajectory τ which forms angle θ_i across line l_i at a distance x_i from p, starting at $i = 0$.*

1. *If $\theta_n = \theta_0$, then τ is periodic and stable.*
2. *Let n be odd. If $\theta_0 = \alpha_1 + \alpha_3 + \cdots + \alpha_{n-2}$, then τ is periodic and stable.*
3. *Let n be even. If $(\alpha_{n-2} - \alpha_{n-1}) + \cdots + (\alpha_2 - \alpha_3) + (\alpha_0 - \alpha_1) = 0$, then any non-escaping trajectory is periodic and stable. If not, every trajectory escapes.*

Proof. Fix a P_n-star with P_n of size zero (so that $p = P_n$ is a point). The trajectory τ cannot enter the "central zone" of P_n, because that is just the point p.

1. If n is even, then Proposition 2.12 applies to τ directly. If n is odd, consider the perturbed trajectory τ'. then $x_{2n}(\tau')$ differs from $x_0(\tau')$ by a linear combination of the z_is. However, $z_i = 0$ for all i, meaning τ' is periodic. In either case, τ is stable.
2. By Theorem 2.13, $\theta_n(\tau) = \theta_0(\tau)$. By 1., The trajectory is periodic and stable.
3. If $n \geq 4$, Theorem 2.16 applies directly to any trajectory. If $n = 2$, then we claim that, if the two lines are perpendicular ($\alpha_0 - \alpha_1 = 0$ implies $\alpha_0 = \alpha_1 = \frac{\pi}{2}$), then any non-escaping trajectory is periodic and stable; if the two lines are non perpendicular, then every trajectory eventually escapes. It is easy to see that Lemma 2.15 applies in this case, as its proof only depends on the angles. And, because the proof of Theorem 2.16 only depends on the angles and on Lemma 2.15, it too applies here.

□

3 Triangle Tilings

Definition 3.1. A *triangle tiling* is a covering of the Euclidean plane with non-overlapping congruent copies of the tiling triangle so that the tiling is symmetric under rotation by π about each vertex.

Lemma 3.2 (Angle Adding Lemma)**.** *Consider a trajectory that consecutively meets the two legs of the tiling triangle that form angle α. If the angle that the trajectory makes with the first leg, on the side away from α, is θ, then the angle that the trajectory makes with the second leg, on the side away from α, is $\theta + \alpha$.*

Proof. If an orbit hits the legs of angle α, then it forms a triangle, where one angle is α and another is the initial angle θ of the orbit. So the exterior angle of the third angle must be $\theta + \alpha$, as shown in Figure 6. □

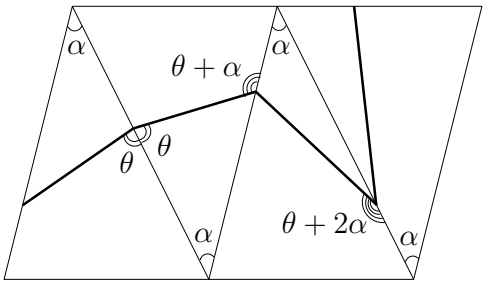

Figure 6: The angle an orbit makes with a leg of a tiling triangle increases by α on the side of the orbit away from the angle α.

Definition 3.3. An orbit is *drift-periodic* if there exist two distinct congruent tiles with the same orientation where the orbit crosses corresponding edges in the same place, at the same angle.

Proposition 3.4. *For each isosceles triangle tiling, all orbits are either periodic or drift-periodic.*

Proof. Call each line containing the bases of the isosceles triangles the *base line*. Note that an isosceles triangle tiling is reflection-symmetric across the base lines, and therefore so are the orbits. So if an orbit crosses the same base line in two places, then it must make a loop upon reflection across that line; the orbit is periodic (Figure 7a). If an orbit crosses two distinct base lines, then upon reflection across either of these lines, the orbit will hit yet another base line, in the same place and at the same angle on the side of a triangle corresponding to the previous place the orbit met a base line (Figure 7b); the orbit is drift-periodic.

Furthermore, every orbit falls into one of these two cases because an orbit cannot travel indefinitely without crossing a base: each time an orbit goes from leg to leg in the tiling, by the Angle Adding Lemma α is added to the angle the orbit makes with the next leg. Eventually, this angle is greater than or equal to $\pi - \alpha$ and the orbit meets a base. So every orbit is either periodic or drift-periodic. □

Proposition 3.5. *For an isosceles triangle tiling with vertex angle α and a trajectory making angle $\theta < \alpha$ with one of the congruent legs, let $n \in \mathbb{N}$ be the unique value such that $\pi - \alpha \leq \theta + n\alpha < \pi$. If n is even, the maximum period of a drift-periodic orbit is $2n + 4$ and the maximum period of a periodic orbit is $2n + 2$; if n is odd, the maximum period of a drift-periodic orbit is $2n + 2$ and the maximum period of a periodic orbit is $2n + 4$.*

Proof. By the definition of n, $\theta + n\alpha$ is the largest angle an orbit can make with a leg before the orbit meets a base line. Suppose that a trajectory meets this maximum number of legs n. If n is even, then the orbit meets another base line after making the angle $\theta + n\alpha$ with a leg and, by the reflection symmetry of the tiling across the base lines, is drift-periodic. By the Angle Adding Lemma and reflection symmetry, a drift-periodic orbit must have $2n$ points where the orbit makes

the angles $\theta + \alpha, \theta + 2\alpha, \ldots, \theta + n\alpha$. Add to this the 4 points when the orbit is traveling to and from a base edge, and the maximum period of a drift-periodic orbit is $2n + 4$. Similarly, the maximum period of a periodic orbit is $2(n - 1) + 4 = 2n + 2$. If n is odd, then the orbit meets a base line a second time after making the angle $\theta + n\alpha$ with a leg and is periodic; the maximum period of a drift-periodic orbit is $2(n-1)+4 = 2n+2$ and the maximum period of a periodic orbit is $2n+4$. □

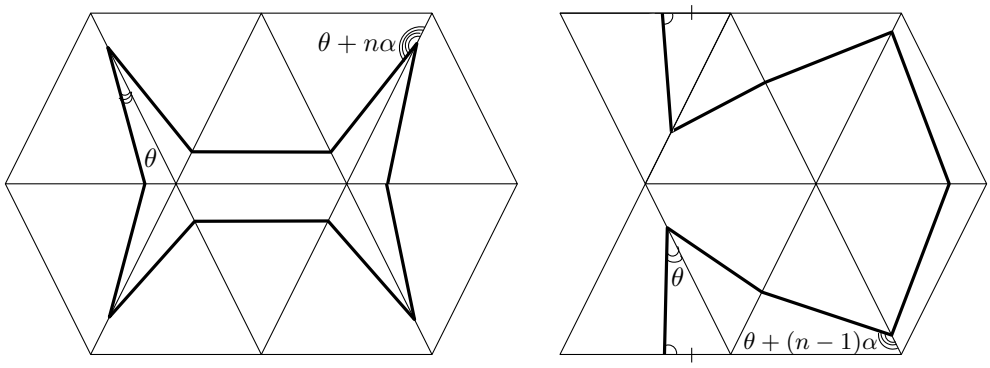

Figure 7: Two orbits in an isosceles triangle tiling: a periodic orbit (left) and a drift-periodic orbit (right). Note that these orbits are reflection-symmetric across the base line.

Notation: We assume that a right triangle tiling is a covering of the Euclidean plane with non-overlapping congruent right triangles so that the tiling has axis-parallel perpendicular edges and the hypotenuses are the negative diagonals of the rectangles formed by the perpendicular edges. We refer to a tiling triangle that lies below its hypotenuse as a *lower tiling triangle*, and to a tiling triangle that lies above its hypotenuse as an *upper tiling triangle*. In any right triangle tiling, α is the smallest angle in the right triangle, and is opposite the horizontal edge. The length of the hypotenuse of the tiling triangle is 1.

Lemma 3.6. *In a right triangle tiling, if an orbit never meets two perpendicular edges in a row, then the orbit is unbounded.*

Proof. Consider an orbit that never meets two perpendicular edges in a row as it passes through a lower tiling triangle, then meets the hypotenuse (Figure 8). The orbit then passes through the upper tiling triangle and crosses either the top or right edge. Either way, it will enter another lower tiling triangle, meet the hypotenuse, then go up or right once again. So the orbit always travels up and right (or in the symmetric case, down and left) and escapes to infinity. □

Proposition 3.7. *In a right triangle tiling, if an orbit bisects a hypotenuse, then the orbit is unbounded.*

Proof. First, we show that if an orbit bisects a hypotenuse, then it bisects the hypotenuse of every tiling triangle it enters.

Let p be the midpoint of a hypotenuse, p' be the reflection of p across the horizontal edge above p, and p'' be the reflection of p' across the vertical edge to the right of p' (see Figure 9). By symmetry, p' is the midpoint of the hypotenuse, and also by symmetry, an orbit through p that crosses the horizontal edge must pass through p'. By a similar argument, p'' is the midpoint of the hypotenuse and an orbit through p' that crosses the vertical edge must pass through p''.

Hence the orbit cannot meet two perpendicular edges in a row; by Lemma 3.6, the orbit is unbounded. □

Lemma 3.8. *If an orbit meets a hypotenuse below (above) its midpoint, the orbit will continue to meet each hypotenuse below (above) its midpoint until it meets two perpendicular edges in a row, at which point the orbit will begin to meet hypotenuses above (below) their midpoints.*

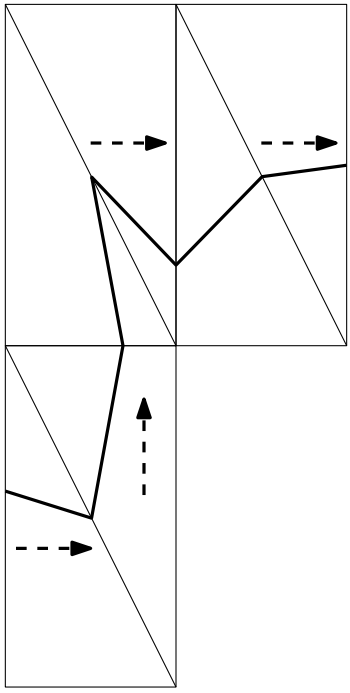

Figure 8: An orbit that never meets two perpendicular edges in a row. Notice that it only travels up and to the right.

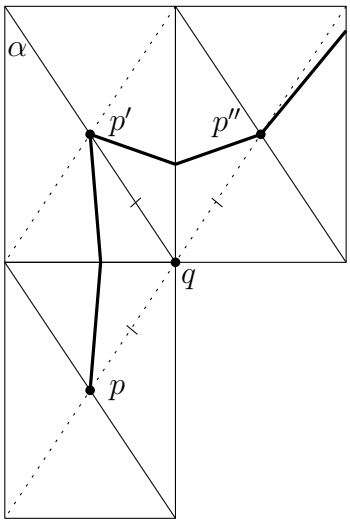

Figure 9: If a trajectory bisects a hypotenuse, it will bisect every hypotenuse.

Proof. Let the orbit meet a hypotenuse below the midpoint in such a way that it next meets a vertical leg, whose lower endpoint is P and upper endpoint is Q, then meets another hypotenuse, whose midpoint we name R (Figure 10). Consider $\triangle PQR$. To meet the hypotenuse above the midpoint, the orbit would have to meet QR. However, this is impossible because, by reflection, the orbit meets PR.

Suppose an orbit meets hypotenuses below the midpoint as described above, but then meets both legs of a tiling triangle before meeting another hypotenuse (Figure 11). Construct the positive diagonals of the tiling. Let p, p', and p'' be the points where the orbit meets the first, second, and third diagonals, respectively, and let q be the shared endpoint of the first and third hypotenuses.

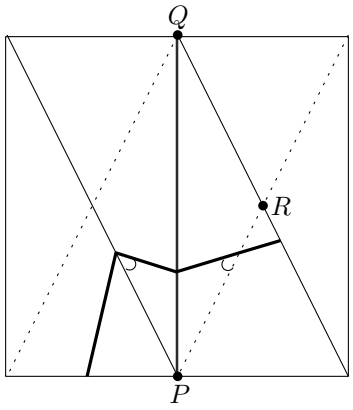

Figure 10: An orbit that meets a hypotenuse below its midpoint will continue to meet hypotenuses below their midpoints.

Let l be the length of the hypotenuses. By symmetry, $|pq| = |qp''|$. So if $|pq| < \frac{l}{2}$, then $|qp''| < \frac{l}{2}$, so the orbit meets the third hypotenuse above the midpoint.

The same argument with the direction of the trajectory reversed applies to orbits meeting the hypotenuse above the midpoint. □

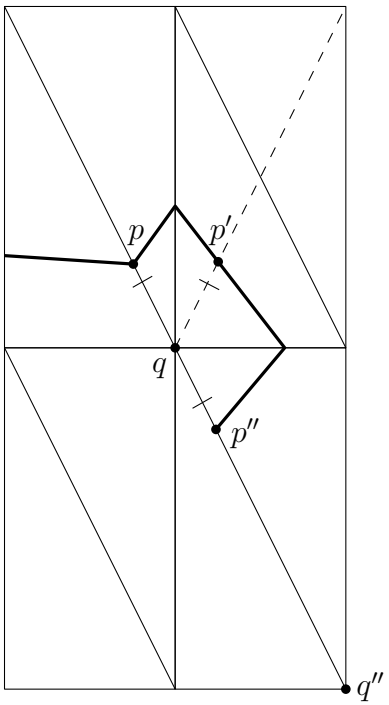

Figure 11: When an orbit meets two perpendicular edges in a row, it switches from meeting hypotenuses below their midpoints (p) to meeting them above their midpoints (p'').

Proposition 3.9. *If α is a rational multiple of π, then there exists $\delta > 0$ such that if an orbit meets a hypotenuse within δ of its midpoint, then the orbit is unbounded.*

Proof. Note that the top and bottom angles at the intersection of the diagonals of a tiling rectangle have measure 2α. Let θ be the angle that the orbit makes at a hypotenuse. The orbit crosses the

edge opposite α if and only if $\theta > \pi - 2\alpha$ because if $\theta = \pi - 2\alpha$, then the orbit meets the corner of the rectangle if it passes through the midpoint of the hypotenuse (see Figure 13).

Case One

Suppose $\theta > \pi - 2\alpha$. An orbit that crosses a hypotenuse below its midpoint with angle θ will make the angle $\theta + 2\alpha - \pi$ at the next hypotenuse it meets (see Figure 12). Let δ be the distance between the orbit and the midpoint of the first hypotenuse. From the law of sines, we see that the distance between the orbit and the midpoint of the second hypotenuse it meets is equal to $\delta_1 = \frac{\delta \sin(\pi-\theta)}{\sin(\theta+2\alpha-\pi)} = -\frac{\delta \sin(\theta)}{\sin(\theta+2\alpha)}$. Note that since $\theta > \pi - 2\alpha$, $\delta_1 > 0$.

Case Two

Suppose $\theta < \pi - 2\alpha$. An orbit that crosses a hypotenuse below its midpoint with angle θ will make the angle $\theta + 2\alpha$ at the next hypotenuse it meets (see Figure 12). Let δ be the distance between the orbit and the midpoint of the first hypotenuse. From the law of sines, we see that the distance between the orbit and the midpoint of the second hypotenuse it meets is equal to $\delta_1 = \frac{\delta \sin(\theta)}{\sin(\pi-\theta-2\alpha)} = \frac{\delta \sin(\theta)}{\sin(\theta+2\alpha)}$. Note that since $\theta < \pi - 2\alpha$, $\delta_1 > 0$.

We induct to find δ_n. Let $k \in \mathbb{N}$. Either $\theta > \pi - 2k\alpha$ or $\theta < \pi - 2k\alpha$. If $\theta > \pi - 2k\alpha$ then suppose $\delta_k = -\frac{\delta \sin(\theta)}{\sin(\theta+2k\alpha)}$. If $\theta < \pi - 2k\alpha$, then suppose $\delta_k = \frac{\delta \sin(\theta)}{\sin(\theta+2k\alpha)}$.

Now, if $\theta > \pi - (2k+2)\alpha$, then by the argument in the base case, $\delta_{k+1} = \frac{\delta_k \sin(\pi-\theta-2k\alpha)}{\sin(\theta+(2k+2)\alpha-\pi)} = -\frac{\delta \sin(\theta)}{\sin(\theta+(2k+2)\alpha)}$.

If $\theta < \pi - (2k+2)\alpha$, then by the argument in the base case, $\delta_{k+1} = \frac{\delta_k \sin(\theta+2k\alpha)}{\sin(\pi-\theta-(2k+2)\alpha)} = \frac{\delta \sin(\theta)}{\sin(\theta+(2k+2)\alpha)}$.

If $\delta_n < \frac{l}{2}$ for all $n \in \mathbb{N}$, where l is the length of the hypotenuse, then our perturbed orbit stays close enough to the bisecting orbit that it will never meet two perpendicular sides in a row and thus, by Lemma 3.6, the orbit will be unbounded. We will prove that this is the case. Since there exists some integer j so that $j\alpha = \pi$, $\sin(\theta + 2k\alpha)$ takes on finitely many values, so we can find $m = \min\{\sin(\theta + 2k\alpha) : k \in \mathbb{N}\}$. So if $\delta < \frac{ml}{2\sin(\theta)}$, then $\delta_k < \frac{l}{2}$ for all $k \in \mathbb{N}$, as desired. □

Proposition 3.10. *If $\alpha = \frac{\pi}{2n}$ for some $n \in \mathbb{N}$, then a drift-periodic orbit exists.*

Proof. Construct an orbit that perpendicularly bisects the short leg of a right tiling triangle (Figure 14). The orbit bisects the hypotenuse of the triangle, meeting it at angle α. By the Angle Adding Lemma, there exists a hypotenuse where the orbit meets at angle $(2n-1)\alpha = \pi - \alpha$. Since the orbit bisects a hypotenuse, by Proposition 3.7, the orbit bisects every hypotenuse it meets, so the orbit perpendicularly bisects the short leg of the upper triangle whose hypotenuse the orbit meets at angle $(2n-1)\alpha$. Since the orbit meets an edge at a corresponding point and at the same angle as where it started, the orbit is drift-periodic. The orbit will also bisect the long leg of a right tiling triangle so we could also begin our construction there, replacing α with $\frac{\pi}{2} - \alpha$ and following the same argument.

□

Conjecture 3.11. *Every rational right triangle tiling has a drift-periodic orbit.*

Proposition 3.12. *Every triangle tiling, except tilings of isosceles triangles with vertex angle greater than or equal to $\frac{\pi}{3}$, has a periodic orbit with period 10.*

Proof. Let α, β be two angles of the tiling triangle and θ be the initial angle the orbit makes with the side of the tiling triangle between α and β, on the α side of the orbit. In Figure 15, we see a ten-periodic orbit for a generic triangle tiling. If each of the labeled angles is positive, then there exists an orbit around two groups of intersecting lines making the angles α, β, and $\pi - \alpha - \beta$. When we add edges so that these intersecting lines become a tiling of triangles with angles α, β, and $\pi - \alpha - \beta$, we can shrink the periodic orbit with period 10 so that it fits within the bounds of the triangles. If we start with a system of inequalities based on every angle in the orbit being positive, we can reduce it to the following system, which implies that a ten-periodic orbit exists:

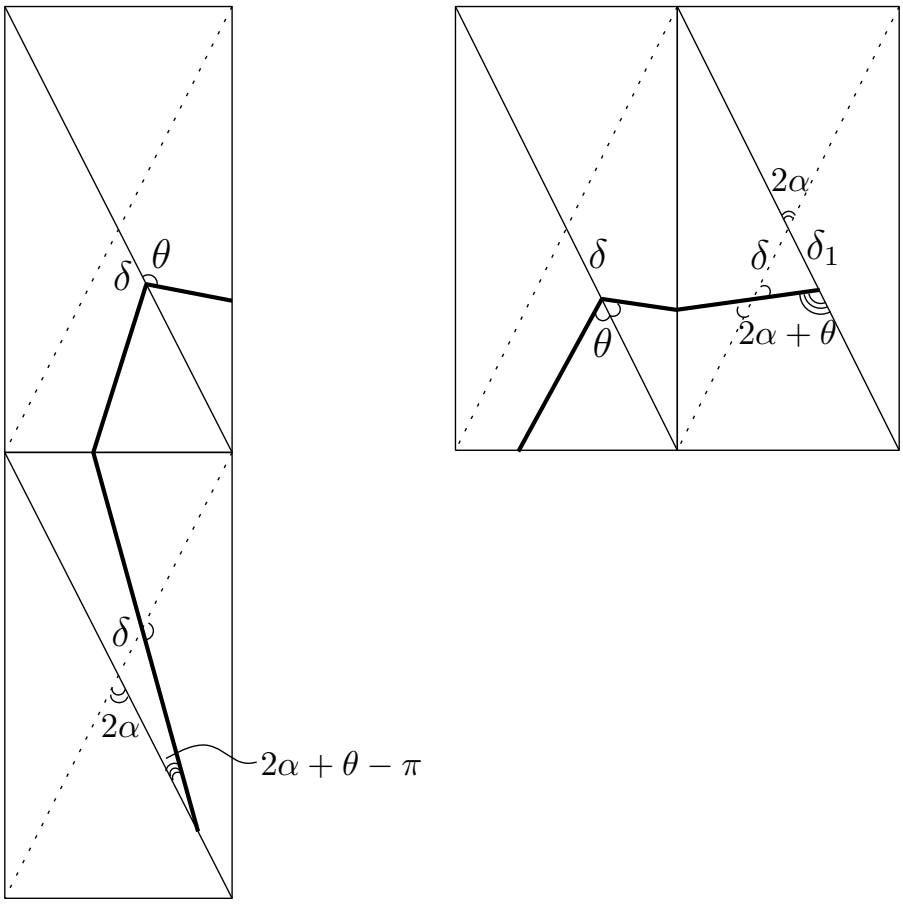

Figure 12: Left: An orbit perturbed by δ from the midpoint of a hypotenuse that meets a horizontal edge between meeting hypotenuses. Right: An orbit perturbed by δ from the midpoint of a hypotenuse that meets a vertical edge between meeting hypotenuses.

$$\begin{aligned} \theta &> 0 \\ \pi - 2\alpha &> \theta \\ \theta &> \beta - 2\alpha \\ 2\beta - \alpha &> \theta \\ \theta &> 2\beta + 2\alpha - \pi \\ \beta + 2\alpha &> \theta \\ \theta &> \alpha. \end{aligned}$$

We can further reduce the system to the following three important inequalities: $\pi > \beta + 2\alpha$, $\frac{\pi}{3} > \alpha$, and $\beta > \alpha$, graphed in Figure 16.

In Figure 16, we see the region of values of α and β where there exists a periodic orbit of period 10 shaded dark gray, which does not contain its boundaries. Since this region contains all β between 0 and 180 degrees, any scalene triangle tiling has a periodic orbit of period 10. However, this is not so for every isosceles triangle tiling. Isosceles triangles lie on the lines $\alpha = \beta$, $180 = 2\alpha + \beta$, and $180 = 2\beta + \alpha$; the first two lines coincide with the boundaries of the region where there exists a periodic orbit of period 10. The third and dotted line is contained in the region of acceptable values when $60 < \beta < 90$ and $\alpha < 60$. In other words, an isosceles triangle only has a ten-periodic orbit

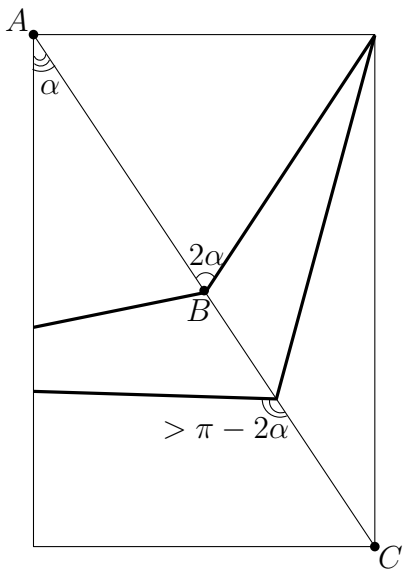

Figure 13: If an orbit crosses the top of the rectangle, then it must make an angle greater than $\pi - 2\alpha$ with the hypotenuse. Note that $AB = BC$.

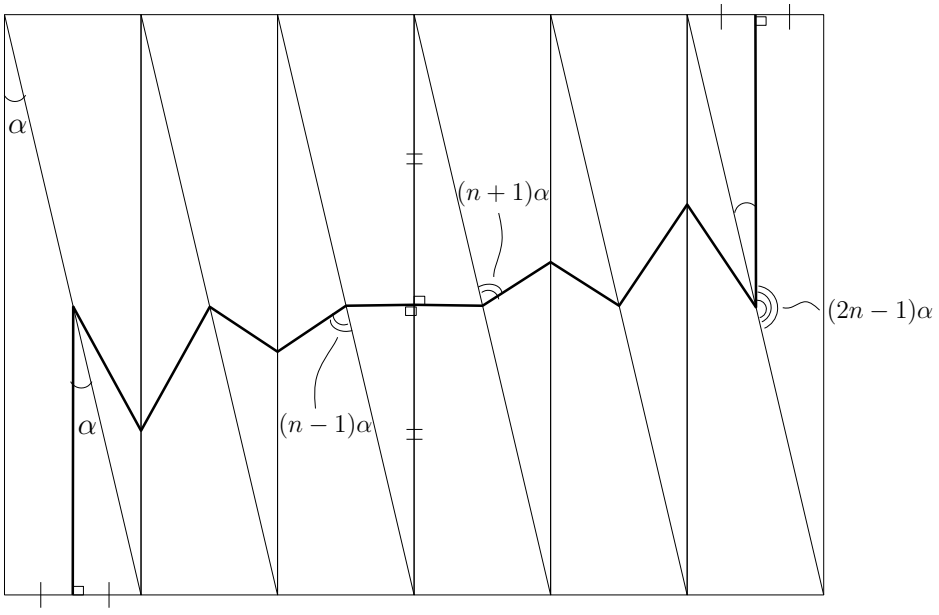

Figure 14: An orbit that perpendicularly bisects the legs of a right tiling triangle must be drift-periodic if $\alpha = \frac{\pi}{2n}$, $n \in \mathbb{N}$.

if its vertex angle is less than $\frac{\pi}{3}$ and a base line of the tiling must cross the interior of the periodic orbit of period 10.

Constructing a Periodic Orbit of Period Ten:

Through repeated application of the law of sines, we see that we obtain a ten-periodic orbit by choosing a value for l, the distance of the orbit from the vertex of angle β along the side between α and β where the orbit makes the angle θ (Figure 15), such that our system of inequalities holds.

For example, if $\alpha = \frac{\pi}{5}$ and $\beta = \frac{3\pi}{10}$, then θ must be between $\frac{\pi}{5}$ and $\frac{2\pi}{5}$. Let $\theta = \frac{3\pi}{10}$. Then $\csc(\frac{3\pi}{10}) - \frac{\sin(\frac{\pi}{10})}{\sin(\frac{3\pi}{10})} = \frac{25-9\sqrt{5}}{11} < l < \frac{16-4\sqrt{5}}{11} = \csc(\frac{3\pi}{10})$.

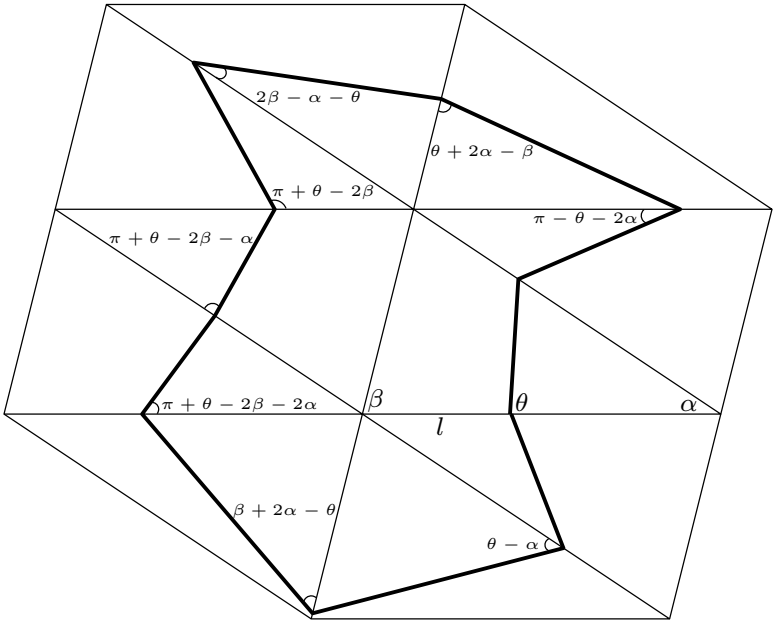

Figure 15: If each of the labeled angles is positive, then this ten-periodic trajectory exists.

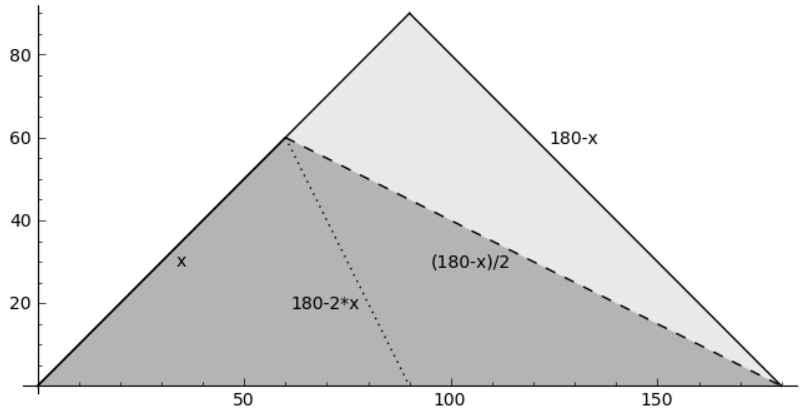

Figure 16: The system of inequalities $\pi > \beta + 2\alpha, \pi > 2\beta + \alpha$, and $\beta > \alpha$, graphed in degrees, with β on the horizontal axis, α on the vertical axis. The light gray region represents all possible triangles with $\beta > \alpha$. The dotted line, $180 = 2\beta + \alpha$, represents the set of α, β where an isosceles triangle has a ten-periodic orbit.

Conjecture 3.13. *There exist triangle tilings with periodic orbits of arbitrary length.*

For instance, the triangle tiling with angles $8°, 79°$, and $93°$ has a periodic orbit of period 34.

Conjecture 3.14. *In a triangle tiling, every periodic orbit has an even period.*

Conjecture 3.15. *In a triangle tiling, no periodic orbit has a period that is divisible by four.*

□

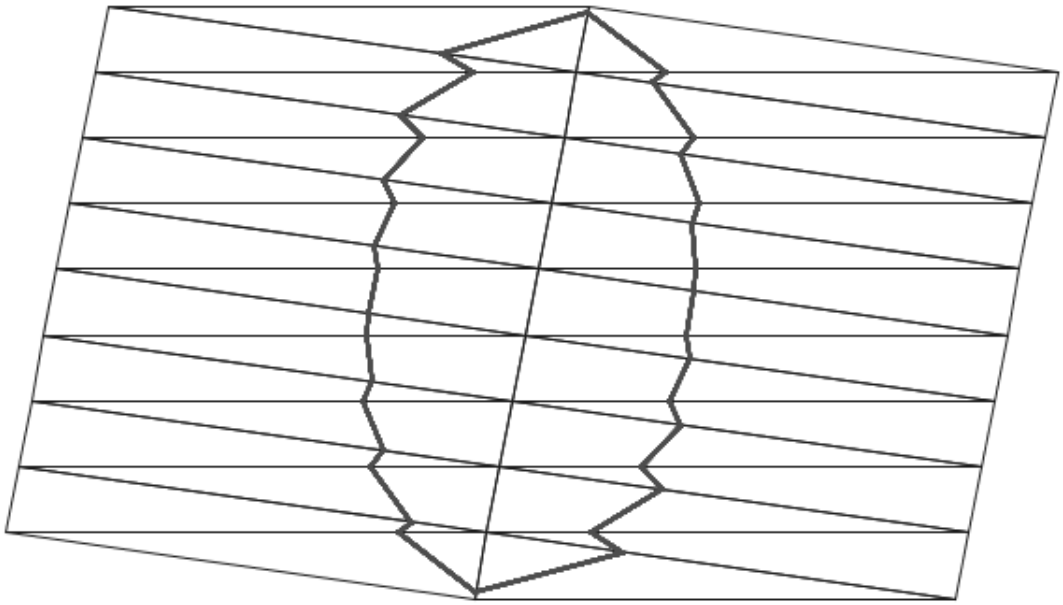

Figure 17: The triangle tiling with angles $8°, 79°$, and $93°$ has a periodic orbit of period 34.

4 The Trihexagonal Tiling

The equilateral triangle tiling and regular hexagon tiling have dynamics that can be easily understood and broken into a few cases. However, the composition of these two tilings into the regular trihexagonal tiling offers a myriad of interesting dynamics. Our goal has been to find the periodic orbits and drift periodic orbits, of the trihexagonal tiling and analyze the stability of these orbits. We begin by analyzing common trajectory paths in the orbits. We will use Lemmas 4.1,4.2,4.3,4.4 to prove the perodicity of orbits.

Lemma 4.1. The Trajectory Turner *Consider a trajectory crossing the edges of the tiling at p_1, p_2, p_3, p_4 where segments $\overline{p_1p_2}$ and $\overline{p_3p_4}$, lie in distinct triangles, segment $\overline{p_2p_3}$ lie in the hexagon adjacent to both triangles, and all three tiles coincide at vertex q. Let the distance from p_i to q be x_i. Then $x_1 = x_4$.*

Proof. Let α be the angle that the trajectory makes at p_1, measured on the same side of the trajectory as q. Then the interior angles at p_2, p_3, p_4 are $\frac{2\pi}{3} - \alpha, \alpha - \frac{\pi}{3}, \pi - \alpha$, respectively. (See Figure **??**).

We use the law of sines to get each x_{i+1} in terms of x_i.

$$\begin{aligned}
\frac{x_1}{\sin(\alpha - \frac{2\pi}{3})} &= \frac{x_2}{\sin\alpha} & \implies x_2 &= \frac{x_i \sin\alpha}{\sin\left(\alpha - \frac{2\pi}{3}\right)} \\
\frac{x_2}{\sin(\alpha - \frac{\pi}{3})} &= \frac{x_3}{\sin\left(\alpha - \frac{2\pi}{3}\right)} & \implies x_3 &= \frac{x_1 \sin\alpha}{\sin\left(\alpha - \frac{\pi}{3}\right)} \\
\frac{x_3}{\sin(\pi - \alpha)} &= \frac{x_4}{\sin\left(\alpha - \frac{\pi}{3}\right)} & \implies x_4 &= \frac{x_1 \sin\alpha \sin\left(\alpha - \frac{\pi}{3}\right)}{\sin\left(\alpha - \frac{\pi}{3}\right)\sin(\pi - \alpha)} = x_1
\end{aligned}$$

as desired. □

Lemma 4.2. The Quadrilateral *In a regular hexagon $ABCDEF$, suppose a trajectory passes from side AB to side CD, crossing AB at a point p_1 and CD at a point p_2. Let $|p_1B| = x_1, |p_2C| = x_2$, and*

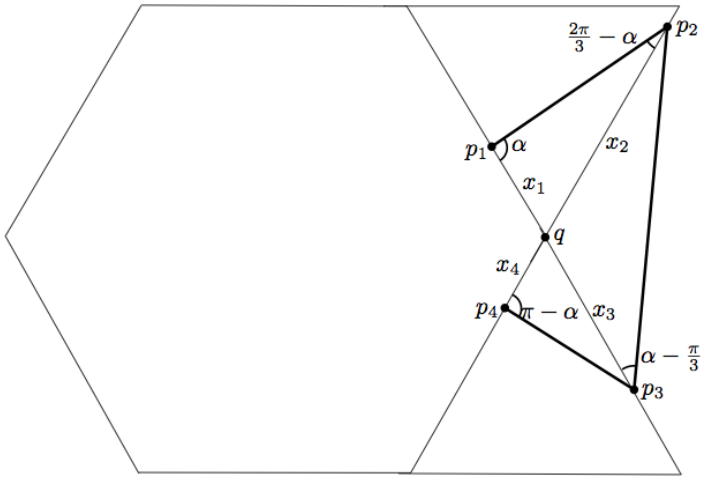

Figure 18: A figure of the Trajectory Turner (Lemma 4.1)

$|BC| = 1$. *If the angle at* p_1*, measured on the same side of the trajectory as* B*, is* $\pi - \alpha$*, then* $x_2 = \frac{\sin(\alpha)(2x_1+1)+\sqrt{3}\cos(\alpha)}{2\sin(\alpha-\frac{\pi}{3})}$.

Proof. Let $|p_1C| = d$ and let $\angle Bp_1C = \beta$, as seen in Figure 19.

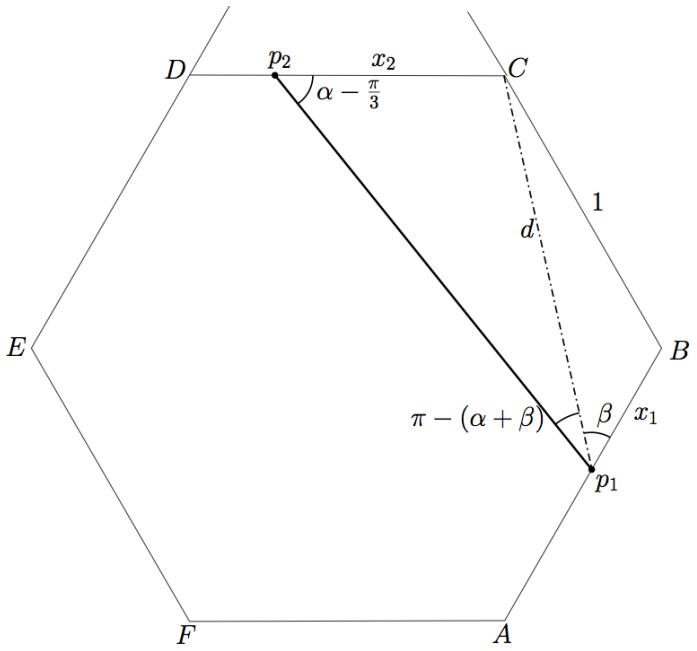

Figure 19: The Quadrilateral

We can use the law of sines to get x_2 in terms of d, α and β:

$$\frac{x_{n+1}}{\sin(\alpha+\beta)} = \frac{d}{\sin(\alpha-\frac{\pi}{3})} \implies x_2 = \frac{d\sin(\alpha+\beta)}{\sin\left(\alpha-\frac{\pi}{3}\right)} = \frac{d\left(\sin\alpha\cos\beta+\cos\alpha\sin\beta\right)}{\sin\left(\alpha-\frac{\pi}{3}\right)}. \tag{1}$$

We can then use the laws of sines and cosines to solve for $\sin(\beta)$ and $\cos(\beta)$ in terms of d to elimate β from equation (1).

$$\frac{1}{\sin\beta} = \frac{d}{\sin(\frac{2\pi}{3})} \qquad \implies \sin\beta = \frac{\sqrt{3}}{2d}$$

$$1 = d^2 + {x_1}^2 - 2dx_1\cos\beta \qquad \implies \cos\beta = \frac{d^2 + {x_1}^2 - 1}{2dx_1} \tag{2}$$

$$d^2 = 1 + {x_1}^2 - 2x_1\cos\left(\frac{2\pi}{3}\right) \qquad \implies d^2 = 1 + {x_1}^2 + x_1 \tag{3}$$

We can now substitute equation (3) into equation (2). This gives us

$$\cos(\beta) = \frac{(1 + {x_n}^2 + x_n) + {x_n}^2 - 1}{2dx_n} = \frac{1 + 2x_n}{2d}$$

We can now substitute our values for $\sin(\beta)$ and $\cos(\beta)$ into equation (1):

$$x_{n+2} = \frac{\sin(\alpha)(1 + 2x_n) + \sqrt{3}\cos(\alpha)}{2\sin(\alpha - \frac{\pi}{3})}$$

as desired. □

Lemma 4.3. *The Quadrilateral-Triangle Give the same setup as in Lemma 4.2, consider equilateral triangle CDT, and suppose that the trajectory intersects side CT at point p_3. Let $x_3 = |p_3C|$. Then $x_3 = \frac{1}{2} + x_1 + \frac{\sqrt{3}}{2}\cot\alpha$.*

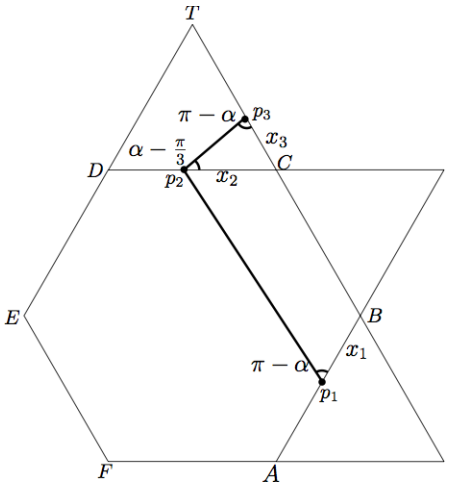

Figure 20: The Quadrilateral-Triangle

Proof. Using the law of sines,

$$\frac{x_2}{\sin\alpha} = \frac{x_3}{\sin\left(\alpha - \frac{\pi}{3}\right)} \implies x_3 = \frac{x_2\sin\left(\alpha - \frac{\pi}{3}\right)}{\sin\alpha}$$

. Applying Lemma 4.2,

$$x_3 = \frac{\sin(\alpha)(2x_1 + 1) + \sqrt{3}\cos\alpha}{2\sin(\alpha - \frac{\pi}{3})}\left(\frac{\sin\left(\alpha - \frac{2\pi}{3}\right)}{\sin\alpha}\right) = x_3 = \qquad \frac{1}{2} + x_1 + \frac{\sqrt{3}}{2}\cot\alpha.$$

□

Lemma 4.4. The Pentagon *In a regular hexagon $ABCDEF$, suppose a trajectory passes from side AF to side CD , crossing AF at a point p_1 and CD at a point p_2. Let $|p_1A| = x_1$, $|p_2C| = x_2$, $|AB| = |BC| = 1$. If the angle at p_1, measured on the same side of the trajectory as A, is $\pi - \alpha$, then $x_2 = x_1 + \sqrt{3}\cot\alpha$.*

Proof. To solve for x_2 we add a segment $\overline{qp_2}$ perpendicular to side AF as seen in Figure 21.
This creates rectangle Aqp_2C. Denote $r = |Aq| = |Cp_2|$ and $s = |AC| = |qp_2|$.
This implies,

$$x_2 = x_1 - t. \tag{4}$$

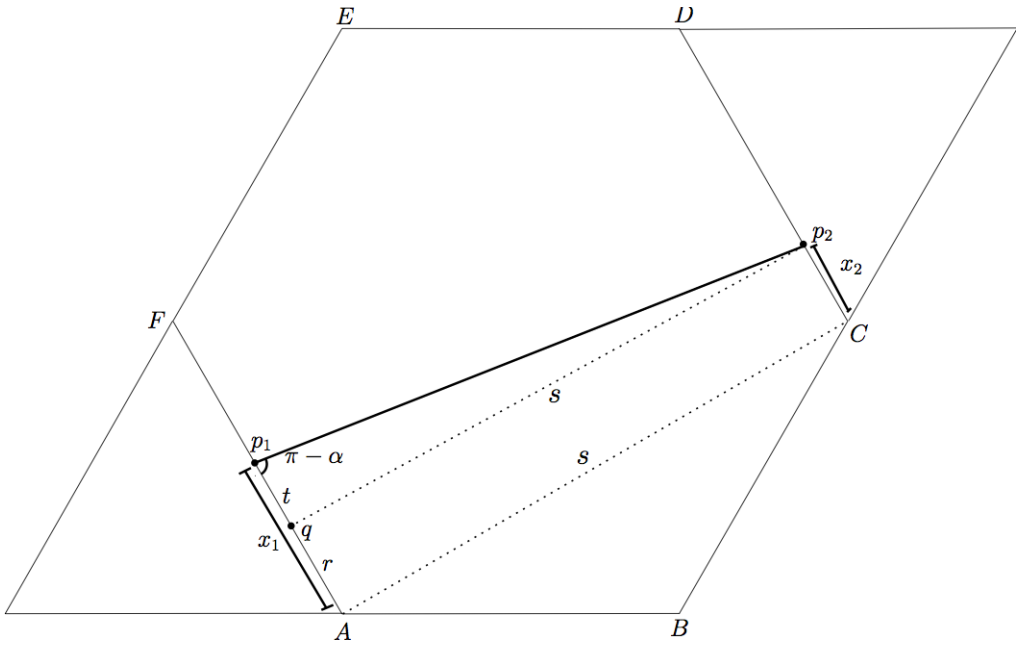

Figure 21: The Pentagon

Because s is the base of an isosceles triangle with vertex angle $\frac{2\pi}{3}$ and equal legs of length 1, $s = \sqrt{3}$. Also, $\tan(\pi - \alpha) = \frac{s}{t}$. So $t = -\sqrt{3}\cot\alpha$.
Now we can solve for t:
Substituting t into equation (4),

$$x_2 = x_1 + \sqrt{3}\cot\alpha \tag{5}$$

□

With the help of these lemmas, we will prove the existence of certain periodic and drift periodic orbits within the trihexagonal tiling.

Theorem 4.5. *There exists a 12-periodic orbit with intial angle $\alpha = \frac{\pi}{2}$.*

Proof. Let $x_1, x_2, x_3, x_4, x_5, x_6, x_7$ be as indicated in Figure 22. By the Trajectory Turner Lemma, $x_1 = x_2$, $x_3 = x_4, x_5 = x_6$. By the Pentagon Lemma, $x_3 = x_2 + \sqrt{3}\cot\frac{\pi}{2} = x_2$. Similarly, $x_4 = x_5$ and $x_6 = x_7$. Thus $x_7 = x_1$, so all x_i's are equal and the trajectory is periodic. □

Remark 4.6. This orbit is stable under parallel translations: As long as the trajectory intersects the edge of the central hexagon perpendicularly, any value of x_1, with $0 < x_1 < \frac{1}{2}$, produces a parallel periodic orbit. An example is shown as a dashed trajectory in Figure 22.

Theorem 4.7. *There exists a 6-periodic orbit intersecting all edges of the tiling at angle $\frac{\pi}{3}$.*

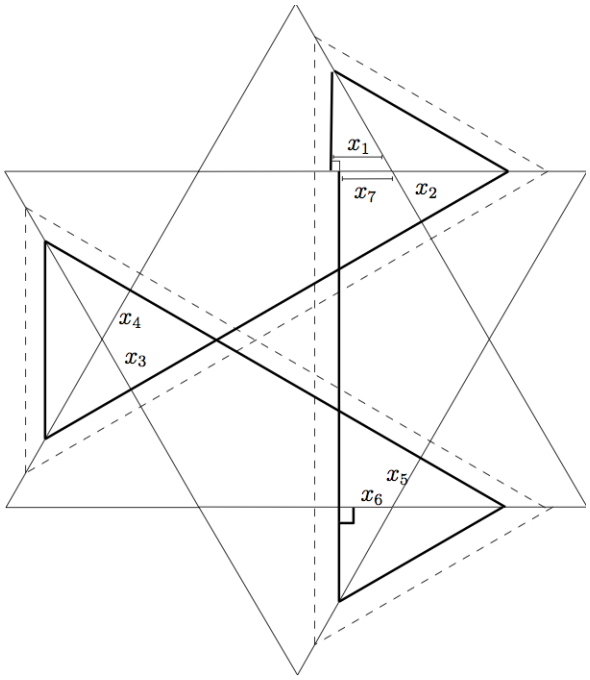

Figure 22

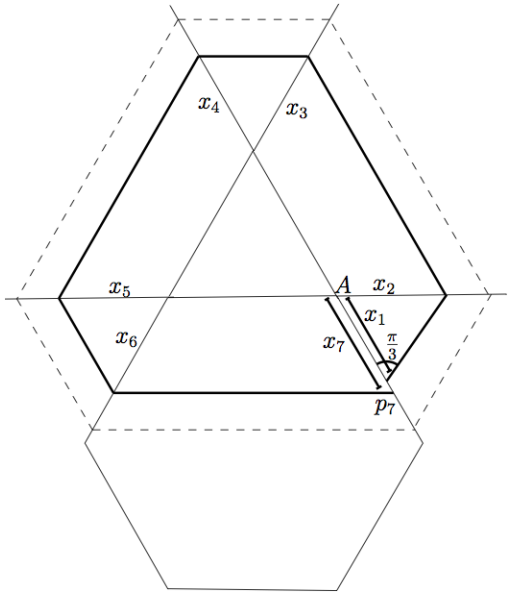

Figure 23: Period 6 orbit

Proof. We can see in Figure 23, that this orbit is covered by Corollary 2.14, because it circles three lines forming a regular triangle, so the proof of Corollary 2.14 along with the unstability of the orbit under angle shifting, applies in this situation as well.

However, it is worth proving why $\alpha = \frac{\pi}{3}$ is the only angle that works for this periodic orbit. Let x_1,...,x_7 be as in Figure 23. Our trajectory is made of equilateral triangles and isoceles trapezoids, so by the triangles $x_1 = x_2, x_3 = x_4, x_5 = x_6$, and using the trapezoids, $x_2 = x_3, x_4 = x_5, x_6 = x_7$. Thus $x_1 = x_7$ as desired. □

Remark 4.8. Like the previous orbit, this orbit is also stable under parallel translations for any $0 < x_1 < 1$. (See figure 23 for a dashed parallel orbit).

Lemma 4.9. *There exists a drift-periodic path with initial angle $\alpha = \pi - \tan^{-1}(3\sqrt{3})$ that intersects each edge of the tiling at most once.*

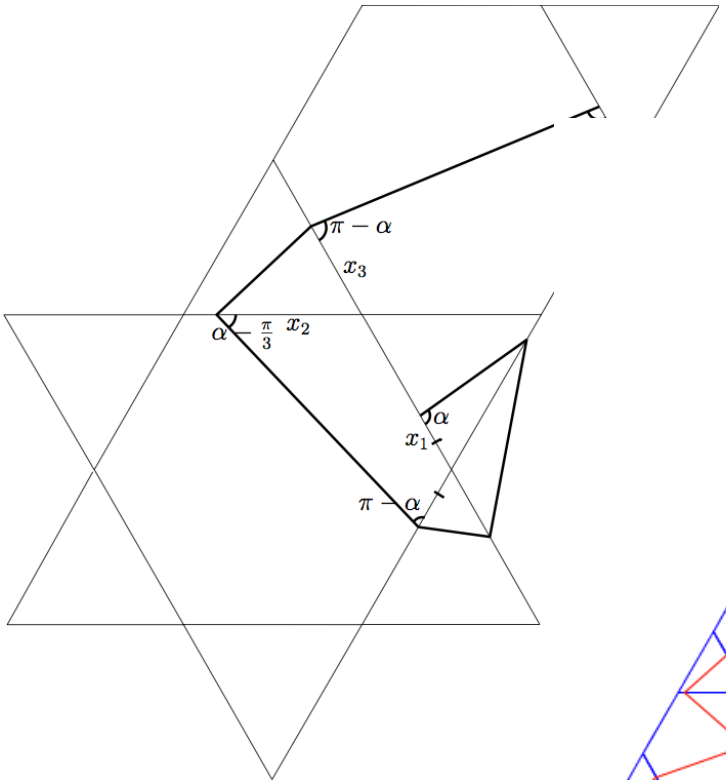

Figure 24: A close up view of the trajectory in Lemma 4.9

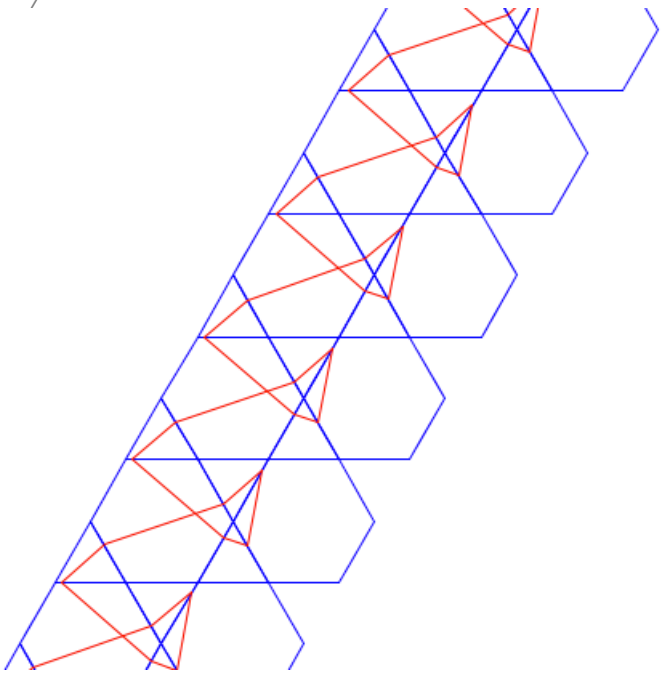

Figure 25: A wide view of the trajectory in Lemma 4.9

Proof. Let x_1, x_2, x_3, x_4 be as in Figure 24.

By Lemma 4.3

$$x_3 = \frac{1}{2} + x_1 + \frac{\sqrt{3}}{2}\cot(\alpha)$$

And by Lemma 4.4

$$x_4 = \frac{1}{2} + x_1 + \frac{3\sqrt{3}}{2}\cot(\alpha) \tag{6}$$

Solving for $\cot\alpha$.

$$\begin{aligned}\alpha =& \pi - \tan^{-1}(3\sqrt{3})\\ \cot(\alpha) =& -\cot(\tan^{-1}(3\sqrt{3})\\ \cot(\alpha) =& \frac{-1}{3\sqrt{3}}\end{aligned}$$

Substituting $\cot\alpha$ into Equation (6):

$$x_4 = \frac{1}{2} + x_1 + \left(\frac{3\sqrt{3}}{2}\right)\left(\frac{-1}{\sqrt{3}}\right) = x_1$$

□

Remark 4.10. Now we will show that the drift-periodic trajectory in Lemma 4.9 is actually the first member of a countable family of drift-periodic orbits.

Theorem 4.11. *Given an trajectory forming an initial angle* $\alpha=\pi - \tan^{-1}((6n-3)\sqrt{3})$ *with* $n \in \mathbb{N}$ *to a side of the hexagon, there exists a drift periodic orbit where n equals the maximum number of intersections to a side of the hexagon.*

Proof. Assume that we have an initial angle of $\alpha = \pi - \tan^{-1}((6n-3)\sqrt{3})$. Let x_1 be the intial starting length of our trajectory from a nearest vertex of the tiling, and let x_{3n+1} be the length of the last segment the first drift-periodic cycle of the orbit, as seen in Figure 26.

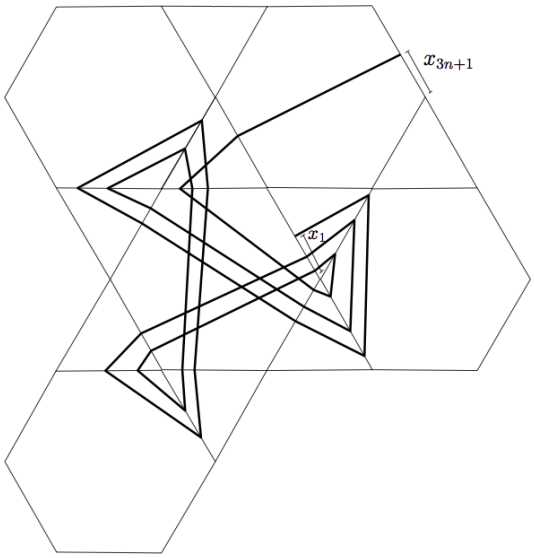

Figure 26: The labelled case of Theorem 4.11 where n = 3.

We want our path to be drift-periodic, which implies that, in order to move from one hexagon to the next, our trajectory must end with Lemma 4.3, proceeded by Lemma 4.4.

From Lemma 4.3

$$x_{3n} = \frac{1}{2} + x_{3n-2} + \frac{\sqrt{3}}{2}\cot\alpha.$$

From Lemma 4.4

$$x_{3n+1} = \frac{1}{2} + x_{3n-2} + \frac{3\sqrt{3}}{2}\cot\alpha.$$

This is the first instance which our trajectory hits the same side of a new translated hexagon to make our trajectory path drift-periodic. Thus no other quadrilaterals have been made by our trajectory, only pentagons and turning trajectories. (See Figures 27,28). This implies

$$x_{3n-2} = x_1 + k\cot(\alpha)$$

for some $k \in \mathbb{N}$.

We write x_{3n+1} in terms of x_1:

$$x_{3n+1} = \frac{1}{2} + x_1 + k\cot\alpha + \left(\frac{3\sqrt{3}}{2}\right)\cot(\alpha) \tag{7}$$

We know that

$$\cot(\alpha) = \frac{-1}{(6n-3)\sqrt{3}}.$$

We want $x_1 = x_{3n+1}$, so we set up (7) to elimate our constants.

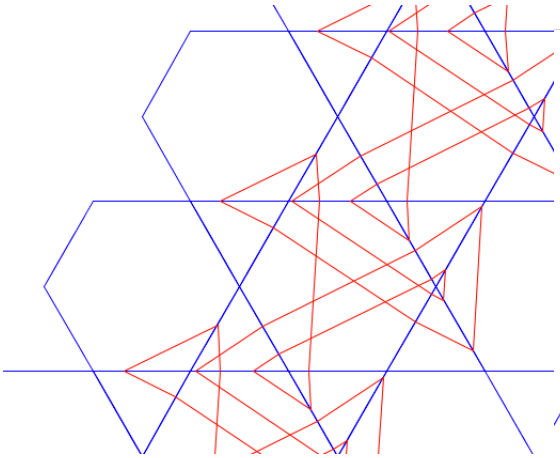

Figure 27: The case of Theorem 4.11 where n = 2

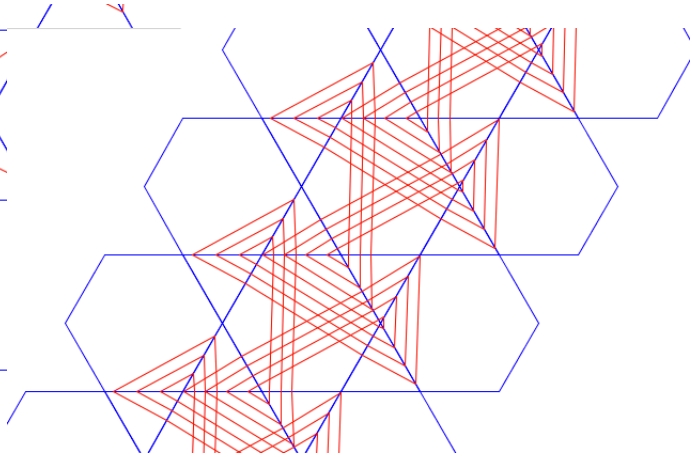

Figure 28: The case of Theorem 4.11 where n= 4

$$\left(\frac{(2k+3)\sqrt{3}}{2}\right)\left(\frac{-1}{(6n-3)\sqrt{3}}\right)+\frac{1}{2}=0$$

$$2k+3=6n-3 \implies k=3(n-1)$$

Thus the value of $k = 3(n-1)$ gives us k pentagons within our orbit. So each side of the hexagon has $(n-1)$ hits from the pentagons formed in the orbit and exactly one more hit to one of the sides from the quadrilateral formed to make the path drift-periodic. This implies that there is at maximum n hits to any side of a hexagon for any drift-periodic path with initial angle $\alpha=\pi - \tan^{-1}((6n-3)\sqrt{3})$. □

Remark 4.12. Like the previous orbits $0 < x_1 < \frac{1}{2}$. Unlike the previous orbits however, these orbits are not completely stable under parallel translations.

Remark 4.13. The limiting value of α is

$$\lim_{n\to+\infty}\alpha=\lim_{n\to+\infty}\pi-\tan^{-1}((6n-3)\sqrt{3})=\frac{\pi}{2}$$

This implies that these drift-periodic orbits are converging to the periodic orbit in Theorem 4.5. So the angles in the drift periodic orbit in Theorem 4.11 are bounded above by $\pi - \tan^{-1}(3\sqrt{3})$ and bounded below by $\frac{\pi}{2}$.

Theorem 4.14. *Given an initial angle $\alpha = \pi - \tan^{-1}(\frac{3n\sqrt{3}}{3n-2})$, then there exists a drift-periodic path where n equals the maximum number of intersections to a side of the hexagon. (See Figure 29).*

Proof. Assume that we have an initial angle of $\alpha = \pi - \tan^{-1}(\frac{3n\sqrt{3}}{3n-2})$. Let x_1, x_{6n-5}, and x_{6n-2} be as in Figure 29. We want our path to be drift-periodic, which implies that, in order to move from one hexagon to the next, we must end with Lemma 4.3, succeeded by Lemma 4.4.

Lemma 4.3 implies,

$$x_{6n-3}=\frac{1}{2}+x_{6n-5}+\frac{\sqrt{3}}{2}\cot\alpha.$$

Then Lemma 4 gives

$$x_{6n-2}=\frac{1}{2}+x_{6n-5}+\left(\frac{3\sqrt{3}}{2}\right)\cot\alpha \tag{8}$$

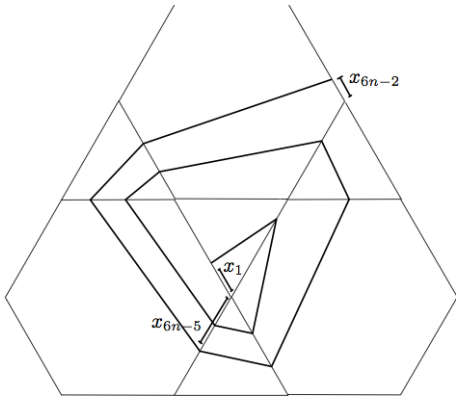

Figure 29: One period of the drift-periodic path in Theorem 4.14 where n = 2.

Solving for $\cot\alpha$ yields,

$$\cot(\alpha) = \frac{2-3n}{3n\sqrt{3}}.$$

From Figure 29, we observe that the trajectory makes the quadrilateral-triangle combination.

So we may apply Lemma 4.3:

$$x_{6n-5} = k\left(\frac{1}{2} + \frac{\sqrt{3}}{2}\cot\alpha\right) + x_1$$

Where k is the number of quadrilateral-triangle combinations. We rewrite equation (8) in terms of x_{6n-2} and x_1.

$$x_{6n-2} = k\left(\frac{1}{2} + \frac{\sqrt{3}}{2}\cot\alpha\right) + x_1 + \frac{1}{2} + \frac{3\sqrt{3}}{2}\cot\alpha \tag{9}$$

We solve for k to get our constants to drop out,

$$\begin{aligned}
\frac{k}{2} + \frac{k\sqrt{3}}{2}\cot\alpha + \frac{1}{2} + \frac{3\sqrt{3}}{2}\cot(\alpha) &= 0 \\
\frac{k+1}{2} + \frac{(k+1)\sqrt{3}}{2}\left(\frac{2-3n}{3n\sqrt{3}}\right) &= 0 \\
k &= 3(n-1)
\end{aligned}$$

This implies that we always have $3(n-1)$ quadrilateral-triangle pairings in the trajectory. These quadrilateral-triangle pairings account for $(n-1)$ intersections to the sides of the hexagon in figure. And one hit is accounted for by the drift-periodic making quadrilateral, therefore we have a drift-periodic path with a maximum of n intersections to the sides of the hexagon. □

Remark 4.15. Like Theorem 4.11, $0 < x_1 < \frac{1}{2}$. Also this orbit is not completely stable under parallel translations.

Remark 4.16. Once again, we can take the limit of α.

$$\lim_{n\to+\infty}\alpha = \lim_{n\to+\infty}\pi - \tan^{-1}(\frac{3n\sqrt{3}}{3n-2}) = \frac{2\pi}{3}$$

This implies that our drift periodic orbit is converging to the periodic orbit in Theorem 4.7. Our angle α is bounded below by $\alpha = \pi - \tan^{-1}(3\sqrt{3})$ and above by $\alpha = \frac{2\pi}{3}$.

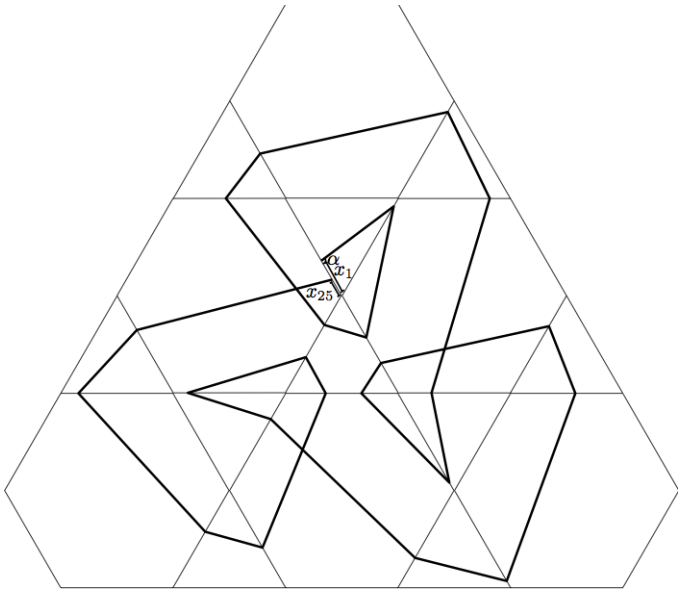

Figure 30: 24-period periodic path

Theorem 4.17. *There exists a 24-period periodic orbit with an intial angle of* $\alpha = \pi - \tan^{-1}(2\sqrt{3})$.

Proof. Define x_1 and x_25 as seen in Figure 30.

From Lemma 4.3, we have

$$6\left(\frac{1}{2} + \frac{\sqrt{3}}{2}\cot\alpha\right) + x_1.$$

From Lemma 4.4, we have

$$x_1 + 3\sqrt{3}\cot(\alpha).$$

So combining these together, we have our equation for x_{25}.

$$x_k = 3 + 6\sqrt{3}\cot(\alpha) + x_1 \tag{10}$$

We solve for $\cot(\alpha)$ to get

$$\cot(\alpha) = \frac{-1}{(2\sqrt{3}})$$

We use our value for $\cot\alpha$ in equation 10.

$$x_k = 3 + 6\sqrt{3}\left(\frac{-1}{(2\sqrt{3})}\right) + x_1 = x_1$$

□

4.1 Conjectures and Open Problems

In right triangle tilings, we showed in Lemma **??** that there exist right triangle tilings such that an orbit starting from a corner will meet a second corner after a certain number of refractions. However, the proof was not constructive. Nevertheless, through computer experimentation, we found a prediction for the values of α, the smallest angle in the tiling triangle.

Conjecture 4.18. *If* $\alpha = \frac{\pi}{2n}$ *and* $\theta + (n-1)\alpha < \pi$, *then an orbit starting from a corner will meet a second corner on the* $n + 1^{st}$ *edge.*

When $\alpha = \frac{\pi}{2}, \frac{\pi}{6}, \frac{\pi}{8}$, or $\frac{\pi}{10}$, it satisfies the corresponding system of equations that guarantees an orbit meets two corners. However, beyond $\frac{\pi}{10}$, we are not aware of a formula for $\frac{\pi}{2n}$, so the problem remains unsolved in the general case.

Larger questions remain open regarding periodic orbits of right triangle tilings. During computer experimentation, we noticed that there appeared to be a bound on the period of an orbit contained in a single row of the tiling (Figure **??**). All periodic orbits observed with larger periods crossed more than one row and remained in each row for the same number of refractions (± 2) as occur in the maximum one-row periodic orbit. However, not every possible number of rows was crossed in a periodic orbit. Thus an open problem is proving that the pattern described above is accurate. The rule predicting how many rows will be crossed in a periodic orbit has also not been found; it is unknown if there is a bound on the periods in a right triangle tiling.

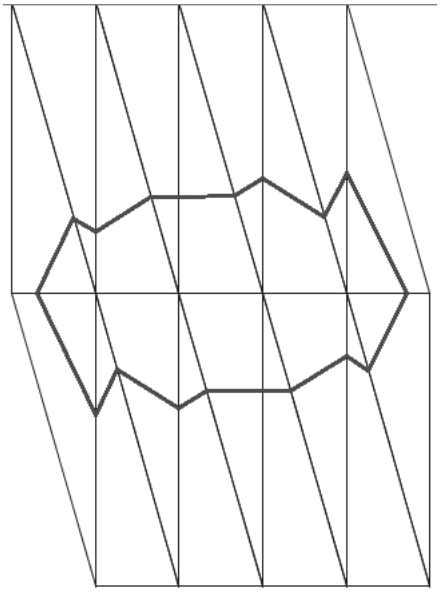

Figure 31: The largest periodic orbit contained in a single row.

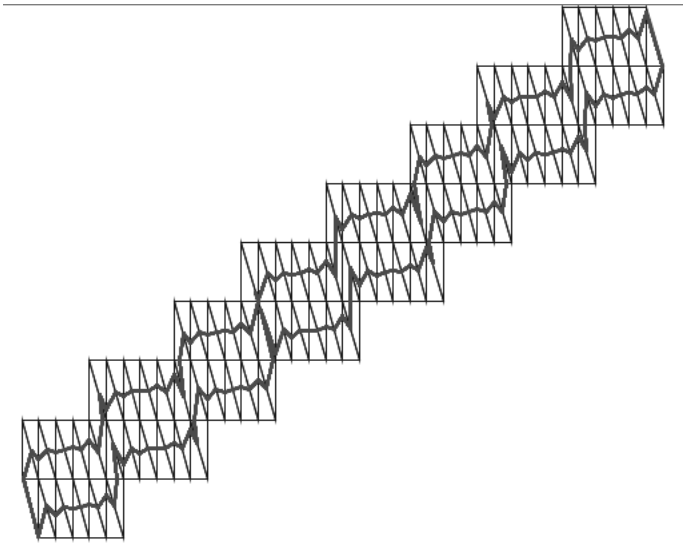

Figure 32: A longer periodic orbit. Note that each row of the periodic orbit resembles the one-row periodic orbit.

Due to its apparent lack of stability, there are still many aspects of the trihexagonal tiling which need to be studied. For example, we were unable to find any stable periodic orbits. It would be worth looking for stable periodic orbits; if none can be found, the question to be proved would be why the trihexagonal tiling cannot support stable periodic orbits.

In addition, as we saw in Theorem 4.14 and 4.11, we have two drift periodic orbits which converge to the periodic orbits in Theorems 23 and 22 respectively. We also found another periodic orbit, as seen in Theorem 4.17. A natural follow up to this discovery of this periodic orbit, is whether there exists a drift periodic path converging to the periodic path in Theorem 4.17. This could possibly be achieved through further experiments and through the methods used within this paper.

Through some additional experiments, we were also able to assemble an array of possibly periodic orbits. Images of these possibly periodic paths can be seen in Figures 33,34,35,36. Due to the incredibly long lengths of the periodic orbits, the methods which we use within in these paper will not suffice for the proofs of these higher level periodic orbits. A pattern for these periodic orbits still is yet to be discovered and subsequently proved. It would also be beneficial to prove whether an upper bound for these periodic orbits has an upper bound. Also, it could be asked whether the possibly periodic paths discussed in the above paragraph also have converging drift periodic orbits.

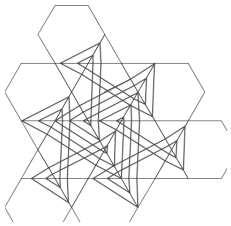

Figure 33: Period 78 Orbit

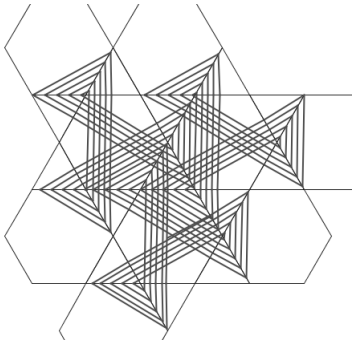

Figure 34: Period 174 Orbit

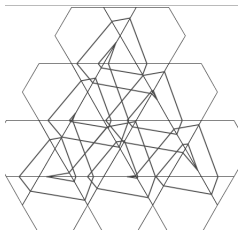

Figure 35: Period 66 Orbit

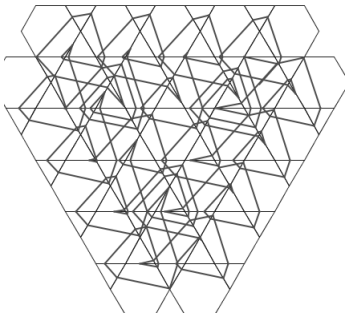

Figure 36: Period 192 Orbit

Outside of the different planar tilings that we considered, one could always consider what types of patterns occur in non-regular tilings. While some of our work in the triangle tiling case looked at non-regular triangle tilings, it would be interesting to consider some more complex tilings, such as the Penrose tiling. In addition, it would be interesting to see if our work could be extended into higher dimensions.

References

[1] A. Mascarenhas, B. Fluegel: *Antisymmetry and the breakdown of Bloch's theorem for light*, preprint.

[2] K. Engelman, A. Kimball: *Negative Snell's Law*, preprint, 2012.

[3] N. Wolchover: *Physicists Close in on 'Perfect' Optical Lens*. Quanta Magazine. 8 Aug 2013.